2015

Driving efficiency in design for rare events using metamodeling and optimization

BOSTON UNIVERSITY

COLLEGE OF ENGINEERING

Thesis

DRIVING EFFICIENCY IN DESIGN FOR RARE EVENTS USING METAMODELING AND OPTIMIZATION

by

PAUL MORRISON

B.Sc., University of Cincinnati, 2011

Submitted in partial fulfillment of the

requirements for the degree of

Master of Science

2015

Approved by

First Reader

Pirooz Vakili, Ph.D.
Associate Professor of Mechanical Engineering
Associate Professor of Systems Engineering

Second Reader

Emily Ryan, Ph.D.
Assistant Professor of Mechanical Engineering

Third Reader

J. Gregory McDaniel, Ph.D.
Associate Professor of Mechanical Engineering

DRIVING EFFICIENCY IN DESIGN FOR RARE EVENTS USING METAMODELING AND OPTIMIZATION

PAUL MORRISON

ABSTRACT

Rare events have very low probability of occurrence but can have significant impact. Earthquakes, volcanoes, and stock market crashes can have devastating impact on those affected. In industry, engineers evaluate rare events to design better high-reliability systems. The objective of this work is to increase efficiency in design optimization for rare events using metamodeling and variance reduction techniques. Opportunity exists to increase deterministic optimization efficiency by leveraging Design of Experiments to build an accurate metamodel of the system which is less resource intensive to evaluate than the real system. For computationally expensive models, running many trials will impede fast design iteration. Accurate metamodels can be used in place of these expensive models to probabilistically optimize the system for efficient quantification of rare event risk. Monte Carlo is traditionally used for this risk quantification but variance reduction techniques such as importance sampling allow accurate quantification with fewer model evaluations. Metamodel techniques are the thread that tie together deterministic optimization using Design of Experiments and probabilistic optimization using Monte Carlo and variance reduction. This work will explore metamodeling theory and implementation, and outline a framework for efficient deterministic and probabilistic system optimization. The overall conclusion is that deterministic and probabilistic simulation can be combined through metamodeling and used to drive efficiency in design optimization.

Applications are demonstrated on a gas turbine combustion autoignition application where user controllable independent variables are optimized in mean and variance to maximize system performance while observing a constraint on allowable probability of a rare autoignition event.

Contents

List of Tables

List of Figures

Chapter 1

Introduction

1.1 Experiment and Optimization in the Design Process

Industrial trends have shifted the system level optimization of hardware to earlier in the design process. This is enabled by better computational tools which more accurately model physical hardware behavior (i.e. computational fluid dynamics, finite element analysis). The objective of this trend is to minimize time and cost of physical experiments by exploring a wider design space (and finding what doesn't work) with minimal impact to overall program schedule and cost. The objective is not to *design* during system level experiments but to *validate* an optimal part or process. The optimal design will have an acceptably small and known level of uncertainty. Table 1.1 describes typical design methods and a qualitative assessment of cost and time required to run.

Computational importance is becoming on par with experiment and theory because accuracy in reproducing physical system behavior has increased. In some cases, computation is replacing experiment because computational fidelity meets or exceeds the objectives of

Cost	**Time**	**Purpose**	**Methods**
0	minutes	establish physics	analytical textbook equations
$	hours	explore design space	multi fidelity computer modeling
$$	days	optimize design / screen	individual component testing
$$$	weeks	verify performance	multi component rig testing
$$$$+	months	validate system interactions	full assembly system level test

Table 1.1: Qualitative Cost & Time for Each Step in the Design Process

the experiment. Both physical experiments and high fidelity computer experiments can be time consuming and resource intensive as shown in Table 1.1 so there is a desire to minimize cost, maximize benefit, and quantify uncertainty. This can be achieved using a simplified mathematical model of the system or process being optimized. The purpose is to numerically represent the physical behavior of a process or system in a manner that can be executed quickly while maintaining a reasonable accuracy of the response.

1.2 Metamodeling in the Design Process

These simplified numerical models are formally referred to as *metamodels* when the basis of the model is a complex computer simulation. For this work, the definition is expanded to include physical experiment data as a complementary basis for the metamodel. This is significant from a stochastic standpoint because complex computer models are deterministic but physical experiment always includes some aspect of bias and error (measurement, setup, etc.). Compared to high fidelity computer models and physical experiment data, metamodels are [25]:

- easier to connect proprietary and expensive simulation codes
- simpler to parallelize
- better able to filter noise
- cover the entire design space
- faster error detection

These characteristics make metamodeling an attractive tool in the design process. They enable rapid exploration of a design space and provide information about a system in locations that have not been tested in a physical experiment or computer simulation. The uncertainty of the information in this unexplored design region can be quantified.

Metamodels can predict unobserved system behavior in two basic ways: interpolating and smoothing. Interpolating refers to the exact reproduction of the response at known data points whereas smoothing refers to the regression based fit of multiple data points without necessarily reproducing the observed result. The smoothing characteristics of

metamodels are attractive for systems which exhibit noisy behavior because the regression acts to smooth out the response and lessening the sensitivity to random noise variation. Response surface methodology falls into the latter smoothing category because the response surface form is polynomial with coefficients determined by least squares regression [26]. On the other end of the interpolation spectrum is the Radial Basis Function metamodel that uses linear combinations of a radially symmetric distance function to exactly reproduce the input data points [26]. Finally, Gaussian Process metamodeling (also known as "kriging") can both exactly interpolate or smooth the dataset based on a covariance function which the designer can control [19]. The engineer must choose the appropriate metamodeling method for their application based on prior knowledge of the system to be modeled. Wang et al. [26] and Simpson et al. [19] provide thorough summaries and suggested applications of many metamodeling techniques.

1.3 Rare Event Simulation Challenges

A rare event is formally defined by Rubino and Tuffin as "an event occurring with a very small probability but important enough to justify their study"[18]. The probability and importance thresholds for rare events vary across domains such as insurance, telecommunications, and transportation.

This work will explore rare event analysis in the context of autoignition. Autoignition is the unintended phenomenon when a fuel air mixture combusts prematurely. An occurrence of autoignition must have a significantly small probability because the consequences of a hardware failure driven by autoignition are very large. For aircraft engine gas turbines, an autoignition event sustained for a certain amount of time may cause hardware damage and subsequent failure of downstream rotating turbomachinery. A representative probability of failure for civil aircraft during a typical flight is one in a billion, or 10^{-9} [18]. For the sake of simplicity in demonstration, this work assumes a maximum probability of an autoignition event to be the same 10^{-9}. Quantifying this probability with physical experiment or high fidelity computational experiment (CFD) requires a prohibitively high number of

evaluations. A an accurate metamodel, coupled with rare event stochastic techniques, is best suited to quantify this risk.

Metamodels are best suited for rare event analysis because they're computationally inexpensive to evaluate while accurately representing system behavior. Metamodels can be evaluated cheaply because they involve simple quadratic equations (in RSM) or matrix inversion (in Gaussian Processes), both being far easier to evaluate than solving complex (flow or mechanical) physics equations for many nodes simultaneously. Rare event analysis requires orders of magnitude more evaluations than traditional Monte Carlo based stochastic analysis which is orders of magnitude more than deterministic optimization. An accurate metamodel is the best vehicle to link these design tools. Figure 1.1 provides an overview of where metamodels and optimization fit in the design process.

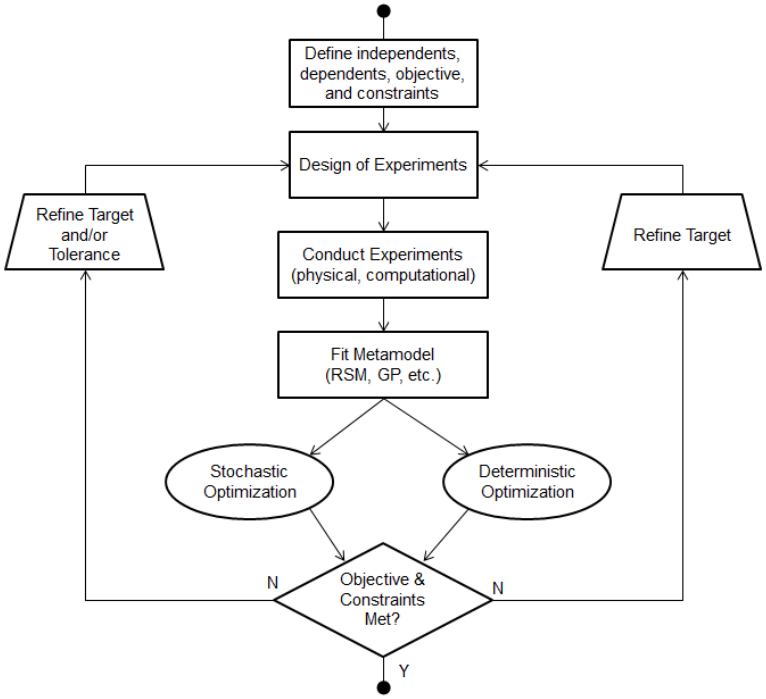

Figure 1.1: Process Framework for Metamodel Enabled Design Optimization

The new contribution of this work is centered on linking deterministic and stochastic optimization for rare events using metamodeling. This unification of metamodeling and

rare event analysis through importance sampling is unique and applicable to efficient design iteration in industry.

1.4 Literature Review and Techniques

The benefits of creating a mathematical surrogate that describes the behavior of a product or process are well established. Many authors have presented methods of building and validating this metamodel surrogate and this work will focus on a subset of those methods useful to an industry practitioner. Meyers and Montgomery [14] present a thorough start-to-finish analysis of Response Surface Methodology (RSM). The framework outlined guides the practitioner through identifying the proper model, fitting the response surface, and basic optimization of the inputs to achieve the desired output of the physical system. Much of the analysis is limited to first and second order parametric models which may not be ideal for all applications.

Guinta [5] provides an application and extension of the RSM framework in his dissertation on high-speed civil transport aircraft design optimization. The work addresses shortfalls of RSM in regards to poor optimization in the presence of numerical noise using a sequential approach. This approach is referred to as Variable Complexity Response Surface Modeling (VCSM) in which the main objective is to narrow the design space with higher fidelity modeling. This allows for a reduction in sampling points and increase in model accuracy because only essential regions of the design space are explored using high fidelity tools.

The stochastic aspects of the RSM framework are outlined by Mavris [10, 11] as Robust Design Simulation (RDS). The method is summarized [10] by :

> RDS combines the response surface model with a Monte Carlo simulation to construct cumulative distribution functions (CDF) and probability density functions (PDF) for the objective and constraints.

RDS differs from deterministic optimization because, instead of absolute maximization of system performance, RDS maximizes performance *and* minimizes the variance of that

maximum performance [11]. The analysis by Mavris et al. [10] is unique in that, in addition to absolute system performance, emphasis is placed on system cost and design risk. Cost and risk can be modeled in the RDS framework (and others) as constraints or additional optimization objectives. This approach is of great interest to the industrial practitioner who must include cost and risk in the business case for a design study.

Wang et al. [26] expand beyond polynomial based RSM into nonparametric models and provide a comprehensive comparison of five metamodeling methods each benchmarked against twenty problems taken from industry or literature. The models are compared for accuracy, flexibility, efficiency, transparency, robustness, and ease of implementation while considering deterministic and probabilistic applications. The authors recommend Radial Basis Functions based on optimal satisfaction of the comparison criteria.

Wang and Shan [25] provide a higher level design process overview of where metamodeling fits in the engineering design process, referred to as metamodel-based design optimization (MBDO). The authors present guidelines on experiment design (sampling) techniques for both physical experiments and stochastic computer analyses. Metamodeling techniques, with emphasis on probabilistic metamodels, and validation strategies of those metamodels are then presented followed by a section on design optimization using the validated metamodel. The optimization strategies are broken into four sections: global, multiobjective, probabilistic, and multidisciplinary. Of particular interest to this work is the probabilistic design optimization strategies. The author concludes that metamodels are best used as surrogates for computationally intense and financially expensive experiments during the design optimization process.

Simpson et al. [19] works through a similar process overview but highlights software applications of metamodeling and design optimization methods in industry. In addition, and most importantly, Simpson et al. uncover common pitfalls when applying statistical regression techniques to deterministic computer simulations, specifically the authors emphasize the difference between bias error due to model fitting and random error inherent in the product or process being modeled. Finally, the authors recommend model choice

based on the characteristics of the product or process the model is intended to represent.

Meckesheimer et al. [12] detail metamodel validation strategies with a specific focus on computational expense. The uncertainty introduced by model bias or random error must be quantified to be managed and the authors present the "leave-k-out" cross validation strategy. Recommendations are made on the value of k for various metamodel types. The authors conclude that the "leave-k-out" cross validation technique provides an adequate balance of model uncertainty quantification with computational expense to determine that uncertainty.

Another approach to quantifying model uncertainty is presented by Donato and Pitchumani [4] entitled QUICKER: Quantifying Uncertainty In Computational Knowledge Engineering Rapidly. The QUICKER method is advantageous because it does not rely on a metamodel but uses a reduced sampling of the full scale simulation to estimate the output distribution of the response. The authors demonstrate a 95% reduction in samples while maintaining accuracy compared to traditional Monte Carlo or Latin Hypercube direct sampling methods.

Chapter 2

Metamodel Theory

2.1 Introduction

At the highest level, a system or process is an observed output characterized by a function of its inputs.

$$y = f(\mathbf{x}) \tag{2.1}$$

where $\mathbf{x} = (x_1, x_2, x_3, \ldots, x_n)^\top$ is the vector of user controllable input variables to the system and y is the observed response. Most real systems or processes also have factors that are uncontrollable by the user yet influence the observed response.

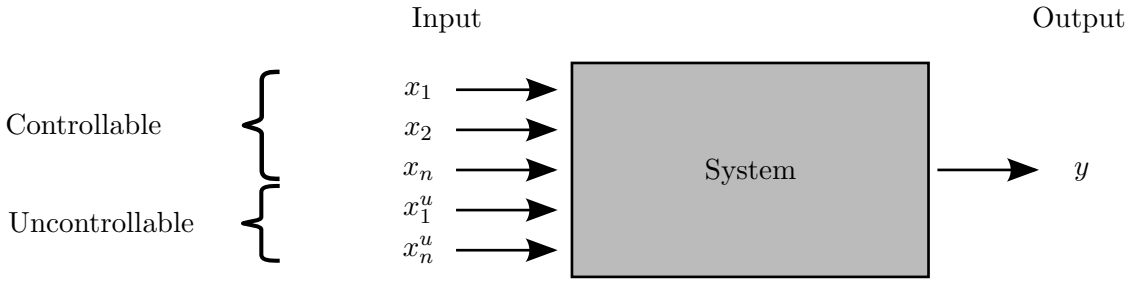

Figure 2.1: *Black Box Approach*

The first objective of modeling is to understand and characterize the behavior of a system. For some simple ideal systems with a few inputs, a pure analytic form of the response is known. However, complex real systems do not have an exact formula for the response as a function of its inputs.

To build a model of a system, the designer must gather data. This can be thought of as a function evaluation at a number of inputs. This function evaluation can be the result of a physical experiment or a computational simulation. The input settings should be chosen

to balance adequate exploration of the design space with cost associated with each function evaluation. For complex systems, each function evaluation can be very expensive. This leads to two critical questions:

1. Where in the design space should the function be evaluated (conduct an experiment, run a simulation)?
2. Given the response at a set of known inputs, how can the response at a different, untested set of inputs be predicted?

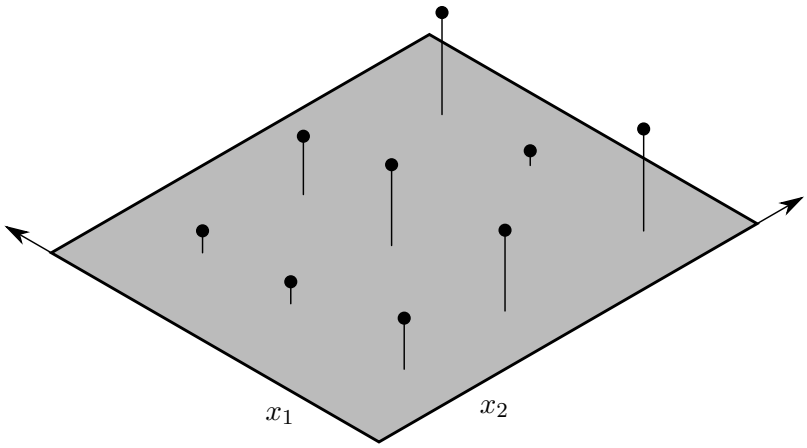

Figure 2.2: *Design Space Function Evaluations*

Question 1 is answered primarily by Design of Experiment (DoE) theory while Question 2 is answered primarily by metamodeling. Yet there are strong interactions between DoE and metamodeling driving an iteration loop.

For this work, physical experiment and high fidelity computer simulation (CFD, FEA, etc.) both provide the same functional evaluation information upon which the metamodel is built. It is accurate to blur the distinction between physical and computer experiment because both can be quite resource intensive to build and run. Whereas running a metamodel requires little computational expense. This blurred distinction is also supported by the effort involved with building the experiment. Creating and assembling physical hardware along with meshing and pre-/post- processing are orders of magnitude more resource intensive than fitting metamodel parameters. Computer simulation is even replacing physical

experiment because simulation accuracy has improved and a more thorough understanding of the system can be obtained using modern computational tools. The philosophy of most high fidelity computer simulation is to duplicate the physical system whereas the philosophy of metamodeling is to accurately predict a single response to a number of known inputs. In addition, high fidelity computer simulation does not scale well. For example, a designer may create a very accurate computer model of a single turbine blade but the engine level sensitivity does not warrant the high computational expense involved in simulating a single turbine blade. Lastly, the low computational expense of a metamodel enables stochastic evaluation and iterative optimization that are prohibitive if run in a physical experiment or high-fidelity simulation.

The second objective of modeling is to find the best values of the user controllable inputs such that the observed response is optimal. Uncontrollable inputs certainly influence the response and the entire field of Robust Design is dedicated to optimizing the controlled inputs to minimize system sensitivity to the uncontrolled inputs.

Uncontrollable inputs may also contribute to system error which is a difference in the observed response from the predicted response. This error is accounted for in metamodeling according to Equation 2.2 [19]:

$$\hat{y} = g(\mathbf{x}) + \epsilon \tag{2.2}$$

where ϵ represents bias and observation error. There is an important distinction between $f(x)$, the underlying physics that govern the system, and $g(x)$ which is the empirical form assumed in metamodeling. There is also an important distinction between y, the true observed response of the system, and $\hat{y}$, the metamodel predicted response of the system. The difference between y and $\hat{y}$ is used to quantify the overall prediction uncertainty of the metamodel. The following sections will outline different empirical forms ($g(\mathbf{x})$) for selected metamodeling strategies.

2.2 Response Surface Methodology (RSM) Theory

This section will focus on a modeling framework called Response Surface Methodology (RSM) which describes the overall process of optimally generating experimental data (historically focused on physical experiment but also adapted to computer experiments), fitting a regression model to that data, and optimizing the inputs to achieve the desired response [14]. This section will focus on the regression model piece of RSM.

The RSM regression model is parametric, meaning there is a known form of the model, and is typically a low order polynomial (first and second order).

$$\hat{y} = \beta_0 + \beta_1 x_1 + \beta_2 x_2 + \epsilon \tag{2.3}$$

$$\hat{y} = \beta_0 + \beta_1 x_1 + \beta_2 x_2 + \beta_{11} x_1^2 + \beta_{22} x_2^2 + \epsilon \tag{2.4}$$

In addition to the isolated input terms, response surface models often include an interaction term to capture response behavior not attributed to a single input alone.

$$\hat{y} = \beta_0 + \beta_1 x_1 + \beta_2 x_2 + \beta_{12} x_1 x_2 + \epsilon \tag{2.5}$$

$$\hat{y} = \beta_0 + \beta_1 x_1 + \beta_2 x_2 + \beta_{12} x_1 x_2 + \beta_{11} x_1^2 + \beta_{22} x_2^2 + \epsilon \tag{2.6}$$

Response surfaces are best visualized in three dimensions with the response plotted on the z axis and two input variables plotted on the x and y axis respectively. Response surface models, however, are not limited to two dimensions but can be applied up to N dimensions.

2.2.1 Taylor Series

The motivation for low order polynomials is first and foremost simplicity in understanding and application. In addition, for a sufficiently narrow region around an observed response, the true function of unknown form can be approximated by a Taylor Series expansion about

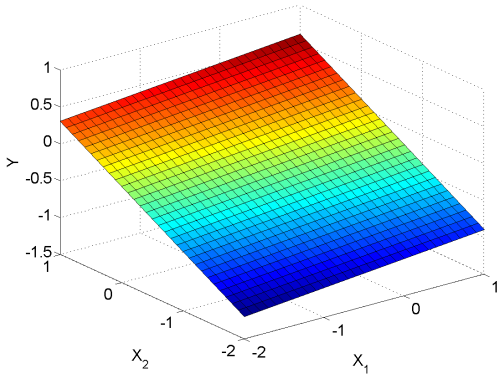

2.3.1: Linear without interaction term

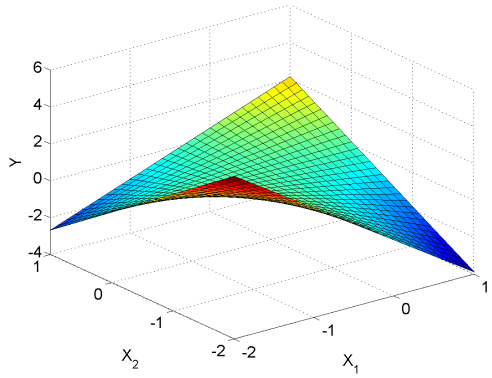

2.3.2: Linear with interaction term

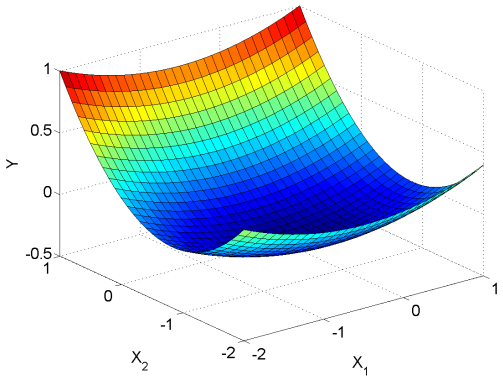

2.3.3: Quadratic without interaction term

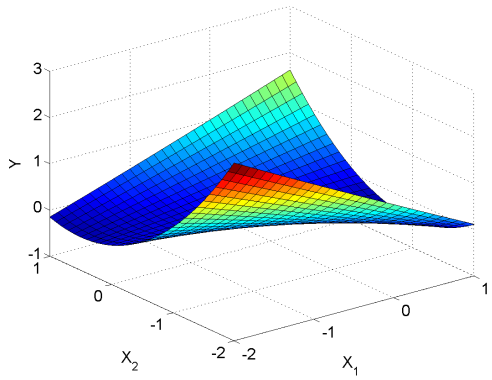

2.3.4: Quadratic with interaction term

Figure 2.3: Response surfaces

a point a.

$$f(x) = f(a) + f'(a)(x-a) + \frac{f''(a)}{2!}(x-a)^2 + \frac{f'''(a)}{3!}(x-a)^3 + ... \tag{2.7}$$

This can be expanded into multiple dimensions where $x_1, x_2, \ldots, x_n$ represents up to n dimensions.

$$f(x_1, \ldots, x_n) = f(a_1, \ldots, a_n) +$$
$$f'(a_1)(x_1 - a_1) + \ldots + f'(a_n)(x_n - a_n) +$$

$$\frac{f''(a_1)}{2!}(x_1 - a_1)^2 + \ldots + \frac{f''(a_n)}{2!}(x_n - a_n)^2 + \\ \frac{f'''(a_1)}{3!}(x_1 - a_1)^3 + \ldots + \frac{f'''(a_n)}{3!}(x_n - a_n)^3 + \ldots \tag{2.8}$$

The Taylor series can be generalized to

$$f(x_1, \ldots, x_n) = f(a_1, \ldots, a_n) + \sum_{j=1}^{n} \sum_{k=1}^{\infty} \frac{f^k(a_j)}{k!} (x_j - a_j)^k \tag{2.9}$$

where n is the dimensionality of the surface and k is the Taylor series order. If the arbitrary system coordinates are shifted such that $a = 0$, the Taylor series reduces to

$$f(x_1, \ldots, x_n) = f(0) + \sum_{j=1}^{n} \sum_{k=1}^{\infty} \frac{f^k(0)}{k!} (x_j)^k \tag{2.10}$$

If the Taylor series is truncated after the second order term

$$f(x_1, \ldots, x_n) = f(0) + \sum_{j=1}^{n} f'(0) x_j + \sum_{j=1}^{n} \frac{f''(0)}{2!} x_j^2 \tag{2.11}$$

If the Taylor coefficients are set equal to the unknown polynomial model coefficients, then the first order polynomial model represents a first-order Taylor series expansion and likewise for second order[14]. Higher accuracy in representing the true response surface can be obtained by introducing higher order polynomial models consistent with carrying more terms in the Taylor series. The engineer is advised against the typical pitfalls associated with increasing order polynomials and over-fitting. The minimum order should be used.

$$\hat{y} = \beta_0 + \sum_{i=1}^{n} \beta_i x_i + \epsilon_i \tag{2.12}$$

$$\hat{y} = \beta_0 + \sum_{i=1}^{n} \beta_i x_i + \sum_{i=1}^{n} \beta_{ii} x_i^2 \tag{2.13}$$

$$\tag{2.14}$$

Because the beta coefficients will be fit based on regression, the engineer can use re-

duction of order techniques to simplify the model form. Using reduction of order, an n dimensional problem can be reduced to a first order polynomial. Myers and Montgomery [14] illustrate reduction of oder with the following example. In the two dimensional second order polynomial in Equation 2.4, let $x_3 = x_1^2$, $x_4 = x_2^2$, $\beta_3 = \beta_{11}$, $\beta_4 = \beta_{22}$, then Equation 2.4 becomes

$$\hat{y} = \beta_0 + \beta_1 x_1 + \beta_2 x_2 + \beta_3 x_3 + \beta_4 x_4 + \epsilon \tag{2.15}$$

2.2.2 Regression Theory

The models built in RSM make use of regression analysis to link observed inputs to predicted outputs. Regression analysis is the act of determining the β coefficients in the above polynomials. Least squares is a common regression method focused on minimizing the sum of the squares of the residual error ϵ between the observed and predicted data. The least squares measure is [14]:

$$E = \sum_{i=1}^{n} \epsilon_i^2 = \sum_{i=1}^{n} \left(y_i - \beta_0 - \sum_{j=1}^{n} \beta_j x_j \right)_i^2 \tag{2.16}$$

It is important to point out the difference between the observed output (y) versus the predicted output ($\hat{y}$). Least squares uses the known values $y = f(\mathbf{x})$ to fit a prediction model $\hat{y} = g(\mathbf{x}) + \epsilon$. For least squares regression, there exists an $n \times 1$ column vector of known observations $\mathbf{y}$ for an $n \times p$ matrix of inputs $\mathbf{X}$ where each row denotes the known inputs for one observation.

$$\begin{bmatrix} y_1 \\ y_2 \\ \vdots \\ y_n \end{bmatrix} = f \left(\begin{bmatrix} x_{11} & x_{12} & \dots & x_{1p} \\ x_{21} & x_{22} & \dots & x_{2p} \\ \vdots & \vdots & \ddots & \vdots \\ x_{n1} & x_{n2} & \dots & x_{np} \end{bmatrix} \right) + \begin{bmatrix} \epsilon_1 \\ \epsilon_2 \\ \vdots \\ \epsilon_n \end{bmatrix} \tag{2.17}$$

This can be rewritten in regression model form as [14]:

$$\begin{bmatrix} y_1 \\ y_2 \\ \vdots \\ y_n \end{bmatrix} = \begin{bmatrix} 1 & x_{11} & x_{12} & \dots & x_{1p} \\ 1 & x_{21} & x_{22} & \dots & x_{2p} \\ \vdots & \vdots & \vdots & \ddots & \vdots \\ 1 & x_{n1} & x_{n2} & \dots & x_{np} \end{bmatrix} \begin{bmatrix} \beta_0 \\ \beta_1 \\ \vdots \\ \beta_p \end{bmatrix} + \begin{bmatrix} \epsilon_1 \\ \epsilon_2 \\ \vdots \\ \epsilon_n \end{bmatrix} \tag{2.18}$$

and in matrix form as:

$$\mathbf{y} = \mathbf{X}\boldsymbol{\beta} + \boldsymbol{\epsilon} \tag{2.19}$$

From Equation 2.16, the sum of the squared error can be rewritten in matrix notation [14]:

$$\begin{aligned} E &= \sum_{i=1}^{n} \epsilon_i^2 = \boldsymbol{\epsilon}'\boldsymbol{\epsilon} = (\mathbf{y} - \mathbf{X}\boldsymbol{\beta})' (\mathbf{y} - \mathbf{X}\boldsymbol{\beta}) && (2.20) \\ &= \mathbf{y}'\mathbf{y} - \mathbf{X}'\boldsymbol{\beta}'\mathbf{y} - \mathbf{y}\mathbf{X}\boldsymbol{\beta} + \mathbf{X}'\boldsymbol{\beta}'\mathbf{X}\boldsymbol{\beta} && (2.21) \\ &= \mathbf{y}'\mathbf{y} - 2\mathbf{X}'\boldsymbol{\beta}'\mathbf{y} + \mathbf{X}'\boldsymbol{\beta}'\mathbf{X}\boldsymbol{\beta} && (2.22) \end{aligned}$$

To minimize the error, its first derivative of E with respect to $\boldsymbol{\beta}$ must be zero. The solution to this zero first derivative equality provides the $\boldsymbol{\beta}$ vector. [14]

$$2\mathbf{X}'\mathbf{y} + 2\mathbf{X}'\mathbf{X}\boldsymbol{\beta} = 0 \tag{2.23}$$

$$\boldsymbol{\beta} = \left(\mathbf{X}'\mathbf{X}\right)^{-1} \mathbf{X}'\mathbf{y} \tag{2.24}$$

2.2.3 VCRSM (Variable Complexity RSM)

Giunta [5] emphasizes the sequential nature of response surface techniques and outlines a design methodology called Variable Complexity Response Surface Methodology. In this technique a response surfaces model is created at a low fidelity and continually refined at increasing levels of fidelity while narrowing the design space until an optimal design is achieved. The response surface model is used primarily as a screening tool to establish minimum performance criteria. The response surface model is also used as an optimization

tool. For a sufficiently narrow design space, the RS is refined based on a few high fidelity experiments at selected points in this narrow design space. This allows optimization methods to have high fidelity knowledge but without the computational expense of repeated high fidelity model evaluation [5]. In addition to the optimization benefits, RS models naturally tend to filter out experimental noise because of the regression fitting procedure. This noise filtering property then lends itself to gradient based optimization techniques which are computationally efficient when operating on a response surface.

Giunta outlines the following steps of the VCRSM Method:

1. Determine the initial design configuration using nominal values from previous experience or intuition.
2. Establish design space boundaries through a lower and upper limit on each independent variable while keeping in mind the physical limitations of the system.
3. Using Design of Experiment theory, establish initial points in the design space to be explored.
4. Conduct a low fidelity analysis at the previously identified points.
5. Reduce the design space by eliminating regions of the design space where constraints are violated.
6. Determine additional points in the reduced design space that meet the D-optimality criterion in DoE theory.
7. Conduct a medium fidelity analysis where the designer evaluates the D-optimal designs chosen in the previous step.
8. Create a metamodel of the system.
9. Optimize the design based on the metamodel. There is significantly reduced computational time to optimize on the metamodel versus medium fidelity model.
10. Analyze the optimal configuration for robustness and validation of optimal design.
11. If design is not deemed optimal, define a new design space, select new boundaries and repeat the previous steps.

Giunta outlines minor variations on the VCRSM method mostly involving determination of design space boundaries.

2.3 Radial Basis Function Theory

The VCRSM method does not restrict the designer to polynomial based response surface metamodels. DACE models (Design and Analysis of Computer Experiments) are another non-parametric class of metamodels which provide flexibility and accuracy advantages at the cost of complexity. Radial Basis Function metamodeling is used when strict interpolation and exact reproduction of known data points is needed. This makes the technique highly desirably for smooth systems that exhibit non-noisy behavior and undesirable for noisy systems. For non-noisy systems, Wang et al. [26] determined that RBF is the most accurate metamodeling technique. Wang et al. also determined that RBF is the most robust technique due to its relative insensitivity to inaccuracy in internal model parameters. At its core, the RBF technique states that points close together in the design space should exhibit similar behavior. This leads to a predictor based on distance between known points. This is best visualized in three dimensions with each point surrounded by a sphere. The sphere surface is the predictor $\phi(r)$ and is only a function of radial distance from the known point $r = |x - x_j|$ [15]. The response prediction is made using linear combinations of the distance from the requested input point to the known response points.

$$y(x) = \sum_{i=1}^{n} w_i \phi(|x - x_i|) \tag{2.25}$$

The still unknown weighting vector ($\boldsymbol{w}$) is determined using the observed responses to known inputs. This imposes the characteristic of RBF that it exactly reproduce the input training set. The procedure for determining $\boldsymbol{w}$ is then reduced to solving a system of n equations for n unknowns [15]. The i subscript below represents unknown quantities and the j subscript represents known quantities.

Name	**Form**
Multiquadratic	$\phi(r) = \sqrt{r^2 + c^2}$
Inverse Multiquadratic	$\phi(r) = \dfrac{1}{\sqrt{r^2 + c^2}}$
Thin-plate spline	$\phi(r) = r^2 \log\left(\dfrac{r}{c}\right)$
Gaussian	$\phi(r) = \exp\left(-\dfrac{1}{2}\dfrac{r^2}{c^2}\right)$

Table 2.1: Alternative Radial Basis Functions [15]

$$y_j = \sum_{i=1}^{n} w_i \phi(|x_j - x_i|) \tag{2.26}$$

Well known linear algebra techniques such as LU decomposition are computationally efficient means to determine the weighting vector.

The radial distance typically assumes the form of a Euclidean norm [26]

$$r = |x - x_j| = \sqrt{(x - x_j)^T (x - x_j)} \tag{2.27}$$

which can be expanded into n dimensions as

$$r = |x - x_j| = \sqrt{\sum_{i=1}^{n} (x_i - x_{ij})^2} \tag{2.28}$$

The basis function $\phi(r)$ itself has several forms, the most common being the multiquadratic function [26]

$$\phi(r) = \sqrt{r^2 + c^2} \tag{2.29}$$

where c is on the order of r and is iteratively determined to minimize prediction error using a "leave-one-out" technique. Other explored functions are summarized in Table 2.1.

Radial Basis Functions are attractive for computational efficiency because the weighting factors and constant must be determined only once allowing subsequent metamodel evaluations (i.e. operating in an optimizer) are very inexpensive.

2.4 Kriging Theory

Modeling a response for uncertain inputs is best handled by the kriging method. Instead of single valued, the inputs are assumed to follow a Gaussian distribution with a known mean and variance. This system of Gaussian inputs is called a Gaussian Process. Kriging is simply another name for Gaussian Process metamodeling after its namesake, D.G. Krige, who applied the method to mining engineering [15].

Kriging has advantages over RS and RBF models because it can interpolate (ie exactly reproduce the input data set) or smooth based on a parameter chosen by the designer. This is because kriging models allow for influence of noise in the observed data. This noise is assumed to be a Gaussian Process (normally distributed) with mean zero and variance σ^2. In matrix notation, the set of observed responses $\mathbf{y}$ is described by some function of the known inputs $\mathbf{x}$ (recall from Section 2.1 $\mathbf{x} = (x_1, x_2, x_3, \ldots, x_n)^\top$), plus a noise term ϵ.

$$y = f(\mathbf{x}) + \epsilon \tag{2.30}$$

$$f(x) \sim \mathcal{N}(\mu, K) \tag{2.31}$$

$$\epsilon \sim \mathcal{N}(0, \sigma^2) \tag{2.32}$$

The GP metamodeling process makes the assumption that the underlying function $f(x)$ can be modeled as a Gaussian Process with mean $\mu(\mathbf{x})$ and covariance $K(\mathbf{x}, \mathbf{x}')$ where $\mathbf{x}$ is the $1 \times n$ vector of n inputs and K is the $n \times n$ covariance matrix. From properties of Gaussian addition, the output y (single observed result plus mean-zero noise, 1×1) can be combined to

$$y = \mathcal{N}(\mu(\mathbf{x}), K(\mathbf{x}, \mathbf{x}') + I\sigma^2) \tag{2.33}$$

where μ is the observed mean vector, I is the identity matrix (since the noise is assumed to be independent), and $K + I\sigma^2$ is the observed covariance matrix (including noise).

The most often used covariance function K in GP regression is the squared exponential function [16]:

$$\operatorname{cov}\left(f(\mathbf{x}), f(\mathbf{x}')\right) = K(\mathbf{x}, \mathbf{x}') = \exp\left(-\frac{1}{2\sqrt{\ell}}|\mathbf{x} - \mathbf{x}'|^2\right) \tag{2.34}$$

Rasmussen and Williams recommend that the $|\mathbf{x} - \mathbf{x}'|$ term above be normalized by a characteristic length term ℓ that the designer may choose to best fit the observed data. This characteristic length and other terms that the designer has control over are called "hyperparameters". These hyperparameters are iteratively determined to minimize the prediction error of the fit by making use of model validation strategies outlined in Section 2.5. The covariance function is referred to in literature as the "kernel" and may take other forms besides the squared exponential function. See Rasmussen and Williams [16] for additional common functions.

To predict the response at a set of unknown values, say $y_{p+1} \dots y_q$, the known input matrix must be identified.

$$\begin{bmatrix} y_{p+1} \\ \vdots \\ y_q \end{bmatrix} = f\left(\begin{bmatrix} x_{(p+1)1} & x_{(p+1)2} & \dots & x_{(p+1)n} \\ \vdots & \vdots & \ddots & \vdots \\ x_{q1} & x_{q2} & \dots & x_{qn} \end{bmatrix}\right) + \begin{bmatrix} \epsilon_{p+1} \\ \vdots \\ \epsilon_q \end{bmatrix} \tag{2.35}$$

For the sake of nomenclature, let $\mathbf{X}_\star$ denote the above $(q-p) \times n$ matrix of inputs for which the unknown, predicted observations are $\mathbf{y}_\star = (y_{p+1} \dots y_q)^\top$. The whole objective of kriging is to find $\mathbf{y}_\star$.

$$\mathbf{y}_\star = f(\mathbf{X}_\star) + \epsilon \tag{2.36}$$

Finally, for the unknown responses, the covariance matrix of the known inputs in matrix notation is $K\left(\mathbf{X}_\star, \mathbf{X}_\star + \sigma^2 I\right)$.

Since the system was assumed to be a Gaussian process, there exists a joint Gaussian observation distribution [16]:

$$\begin{bmatrix} \mathbf{y} \\ \mathbf{y}_\star \end{bmatrix} \sim \mathcal{N}\left(\begin{bmatrix} \mu \\ \mu_\star \end{bmatrix}, \begin{bmatrix} K(X,X) + \sigma^2 I & K\left(X, X_\star\right) \\ K\left(X_\star, X\right) & K\left(X_\star, X_\star\right) + \sigma^2 I \end{bmatrix} \right) \tag{2.37}$$

where K is the matrix of covariances for the inputs with either observed (X) or unobserved $(X_\star)$ output. It is a GP best practice to transform the input data such that the mean μ is zero to produce an unbiased estimator of the response. To ease the nomenclature for the next section, Equation A.5 can be rewritten as:

$$\begin{bmatrix} \mathbf{y} \\ \mathbf{y}_\star \end{bmatrix} \sim \mathcal{N}\left(\begin{bmatrix} \mu \\ \mu_\star \end{bmatrix}, \begin{bmatrix} A & C^\top \\ C & B \end{bmatrix} \right) \tag{2.38}$$

Finally, the conditioning properties of a joint Gaussian distribution allow the distribution of $\mathbf{y}_\star$ to be directly computed[16].

$$\mathbf{y}_\star | \left(\mathbf{y}, \mathbf{X}, \mathbf{X}_\star\right) \sim \mathcal{N}\left(\mathbf{M}, \mathbf{V}\right) \tag{2.39}$$

where

$$\mathbf{M} = \mu_\star + CA^{-1}\left(\mathbf{y} - \mu\right) \tag{2.40}$$

$$= \mu_\star + K\left(X_\star, X\right) K\left(X, X\right)^{-1}\left(\mathbf{y} - \mu\right) \tag{2.41}$$

$$\mathbf{V} = B - CA^{-1}C^\top \tag{2.42}$$

$$= \left[K\left(X_\star, X_\star\right) + \sigma^2 I\right] - K\left(X_\star, X\right)\left[K\left(X, X\right) + \sigma^2 I\right]^{-1} K\left(X, X_\star\right) \tag{2.43}$$

To observe the GP zero mean best practice, the data should be transformed such that $\mu = 0$. This enables an unbiased estimator of $y_\star$ such that $\mu_\star = 0$ as well. Finally,

$$\mathbf{y}_\star | \left(\mathbf{y}, \mathbf{X}, \mathbf{X}_\star\right) \sim \mathcal{N}\Big(K\left(X_\star, X\right) K\left(X, X\right)^{-1} \mathbf{y}, \\ \left[K\left(X_\star, X_\star\right) + \sigma^2 I\right] - K\left(X_\star, X\right)\left[K\left(X, X\right) + \sigma^2 I\right]^{-1} K\left(X, X_\star\right)\Big) \quad (2.44)$$

2.5 Model Validation

The most common model validation strategy is called "leave-k-out" cross validation. The strategy involves leaving a subset (of dimension k) of the full data set (of dimension n) out of the metamodel fitting process and then using this fit to predict the subset of data which was left out.

$$y\left(\begin{bmatrix} N \\ N-k \end{bmatrix}\right) = f\left(\begin{bmatrix} N \\ N-k \end{bmatrix}\right) + \epsilon\left(k\right) \quad (2.45)$$

The difference between the predicted and observed values provides an error quantification of the model. This process can be repeated iteratively over the entire set of observed data. This process is computationally efficient to quantify metamodel accuracy because no new (expensive) computer simulations or physical experiments are required. The full dataset used to fit the metamodel is also used to validate the metamodel [12] driving up the amount of information extracted from a single experiment (experimental efficiency). In addition, "leave-k-out" is a conceptually simple validation strategy which make it attractive for industry practitioners.

Meckesheimer [12] offers strategies for choosing the value of k for several different metamodel types. For low-order polynomials and radial basis functions, a k value of one is recommended. This gives the best error estimate because all of the observed datapoints are being removed one at a time. Leave-one-out is enabled by the ease of which low order polynomials and radial basis functions are re-fit, which must occur n times. According to Meckesheimer, the best choice of k for Gaussian Process (kriging) metamodeling is

$k = 0.1N$. This is due to the optimization loop on the user defined hyperparameters for each validation iteration. For well behaved models, it is a reasonable assumption to hold these parameters constant to avoid this loop and increase efficiency [12].

Chapter 3

Metamodel Test Problems

3.1 One Dimensional Sample Problem

To demonstrate the strengths and weaknesses of the aforementioned metamodeling methods, a simple predictive model of the form

$$y = x^2 \tag{3.1}$$

will be fit for the RSM, RBF, and Kriging techniques. An extension can be made by adding in an artificial error term ϵ to the observed value to become

$$y = x^2 + \epsilon \tag{3.2}$$

Observing the comparisons in Figure 3.1, the 2nd Order Response Surface Model appears to have the best fit. However, this is misleading because the underlying form of the observed values is also second order. For the practitioner, this underlying form is rarely known and rarer still does it exactly match the assumed form of the metamodel.

To demonstrate a more realistic (but still simple and one dimensional) problem, the following is used to demonstrate again the various metamodeling approaches. This function is non-monotonic.

$$y = 2\sqrt{x} + \cos(x) + \epsilon \tag{3.3}$$

Again, observing the comparisons in Figure A.3, the true function is much better pre-

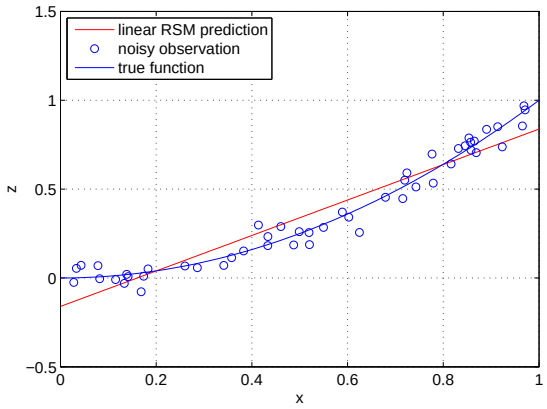

3.1.1: Linear RSM

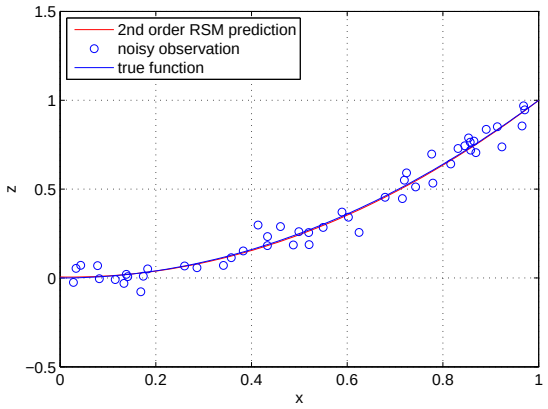

3.1.2: Second Order RSM

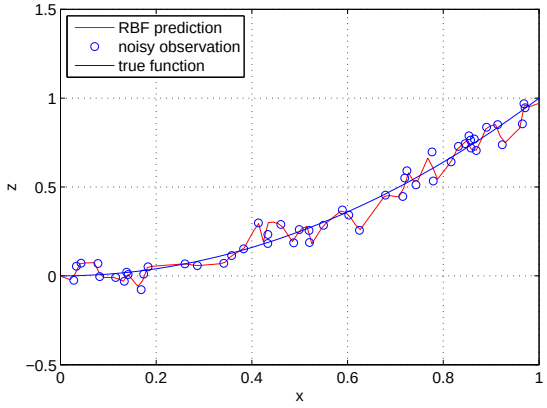

3.1.3: RBF

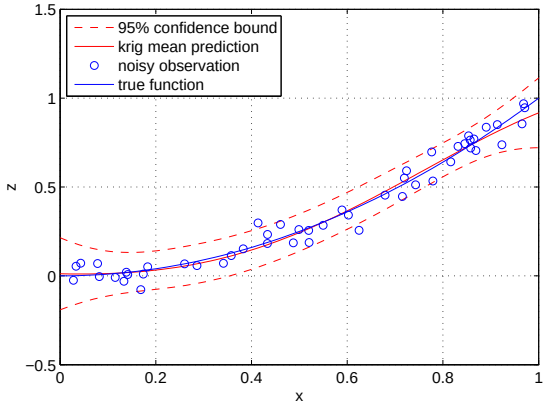

3.1.4: Kriging

Figure 3.1: Noisy Metamodeling for $y = x^2 + \epsilon$

dicted by the Radial Basis Function and kriging methods. Recall, the major difference is that RBF is exactly interpolative, meaning the predicted model will exactly pass through all of the observed datapoints. Whereas, the kriging approach will attempt to accommodate the error in the observation. The other distinct advantage of kriging is that it also provides a variance on the prediction which is very important for unexplored regions of the design space.

3.2 Two Dimensional Sample Problem

To further expand the realism of these examples, the non-monotonic one-dimensional example is expanded into a second input dimension.

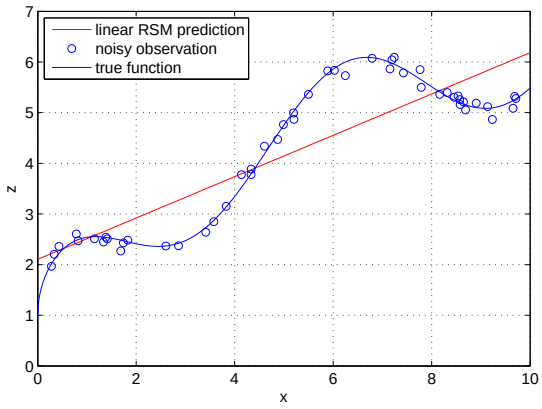

3.2.1: Linear RSM

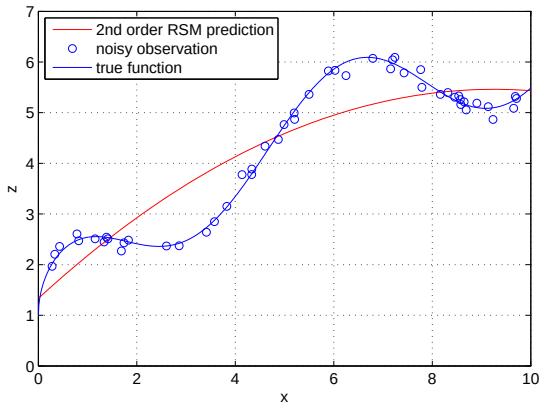

3.2.2: Second Order RSM

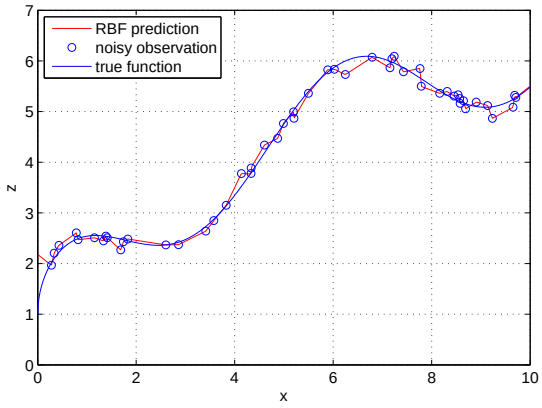

3.2.3: RBF

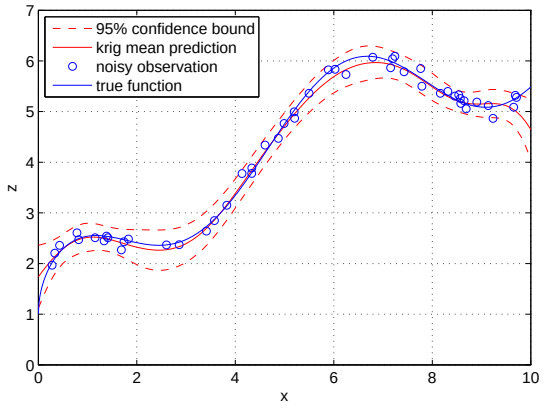

3.2.4: Kriging

Figure 3.2: Noisy Metamodeling for $y = 2\sqrt{x} + \cos(x) + \epsilon$

Again, observing the comparisons in Figure 3.3, Kriging has the best visual representation of the underlying data.

3.3 Error Analysis

For the sample problems in the previous section, visually inspecting the model for best fit isn't adequate. The degree to which the model fits the data must be quantified. A widely accepted measure of model fit is the coefficient of determination or R^2. This coefficient is defined in terms of the sum squared error due to model fitting (residuals) versus the total sum of squares.

$$R^2 = 1 - \frac{SS_E}{SS_T} \tag{3.4}$$

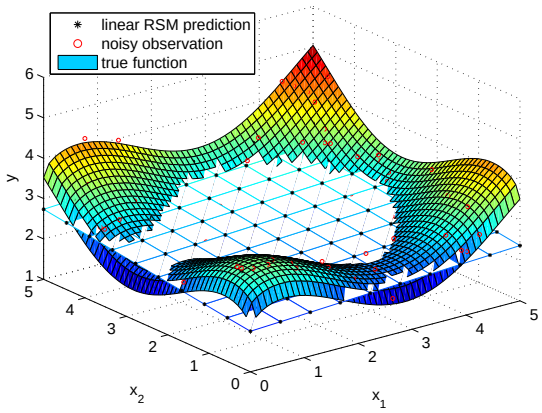

3.3.1: Linear RSM

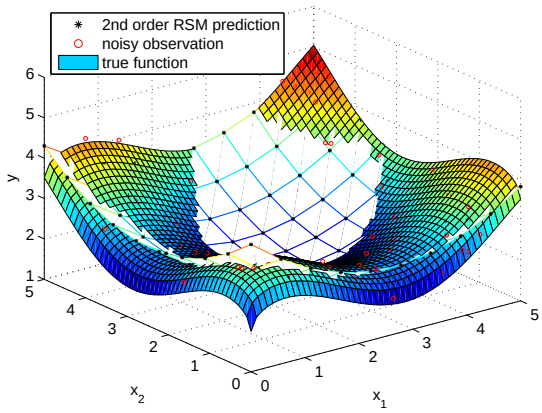

3.3.2: Second Order RSM

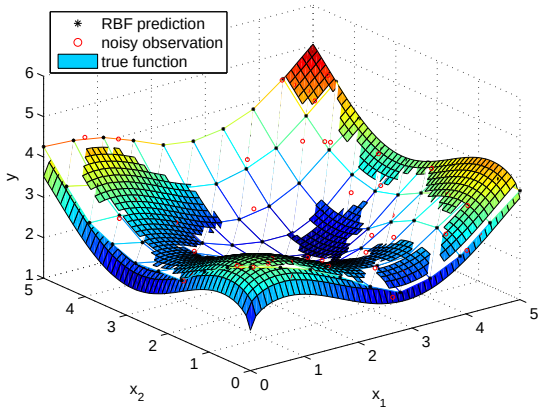

3.3.3: RBF

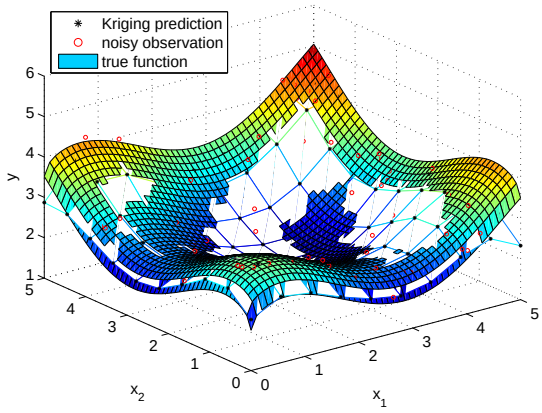

3.3.4: Kriging

Figure 3.3: Noisy Metamodeling for $y = \sqrt{x_1} + \sqrt{x_2} + \cos(x_1) + \cos(x_2) + \epsilon$

where

$$SS_E = \sum_{i=1}^{n} y_{\text{obs},i}^2 - \sum_{i=1}^{n} y_{\text{pred},i}^2 \tag{3.5}$$

$$SS_T = \sum_{i=1}^{n} y_{\text{obs},i}^2 - \frac{\left(\sum_{i=1}^{n} y_{\text{obs},i}\right)^2}{n} \tag{3.6}$$

R^2 may be skewed by overfitting since the value will always increase as more terms are added to the model [14]. Meyers and Montgomery suggest using an adjusted R^2 which will

actually decrease when non-essential terms are added to the model.

$$R^2_{adj} = 1 - \frac{n-1}{n-p}\left(1 - R^2\right) \tag{3.7}$$

Another measure by which models are assessed is the normality of residuals. The best model will have residuals normally distributed with mean zero and minimal variance σ^2_{res}. Table 3.1 summarizes the fit statistics for the above sample problems. The residual mean for all of the cases was very near zero. The residual normality plots can be found in Appendix B.1.

The metamodel with the least predictive error is usually Kriging (based on the residual variance). The exception is for the 1D case of $y = x^2$ where the second order response surface had a marginally lower variance. This is unlikely to propagate to practical applications since the underlying form of the noisy function exactly matches the guessed form of the response surface. Radial basis functions exactly replicate the input data which is undesirable for cases with known noise.

	Model	R^2	R^2_{adj}	σ^2_{res}
1D x^2	Linear RSM	0.9144	0.9126	0.0087
	Second Order RSM	0.9716	0.9704	0.0029
	RBF	1.0	-	-
	Kriging	0.9436	-	0.0030
1D $2\sqrt{x} + \cos x$	Linear RSM	0.7845	0.7800	0.4250
	Second Order RSM	0.8482	0.8418	0.2993
	RBF	1.0	-	-
	Kriging	0.8123	-	0.0131
2D	Linear RSM	0.1264	-0.1232	0.4353
	Second Order RSM	0.8263	0.6092	0.0865
	RBF	1.0	-	-
	Kriging	0.6928	-	0.0110

Table 3.1: Fit Statistics for Sample Metamodel Problems

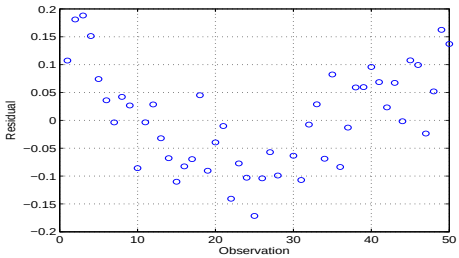

3.4.1: Linear RSM

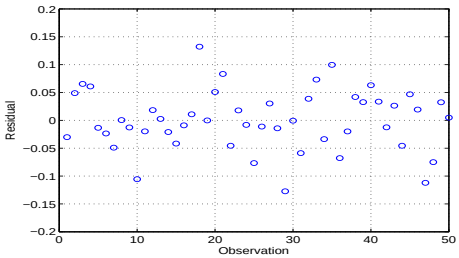

3.4.2: Second Order RSM

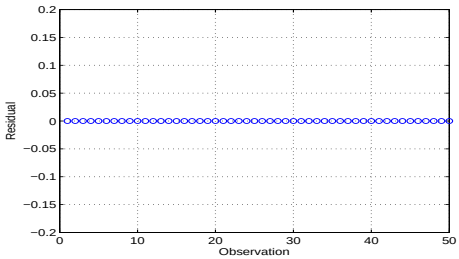

3.4.3: RBF

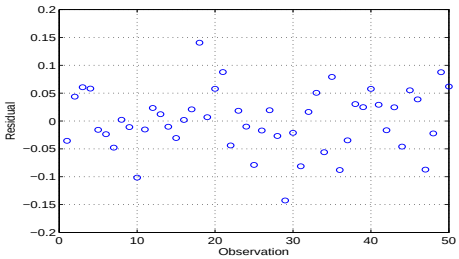

3.4.4: Kriging

Figure 3.4: Residual Plots for $y = x^2 + \epsilon$

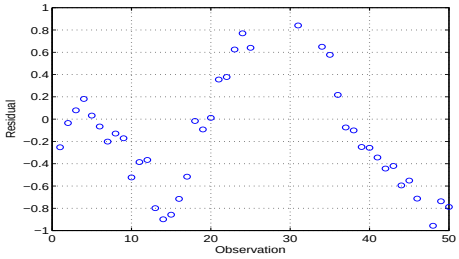

3.5.1: Linear RSM

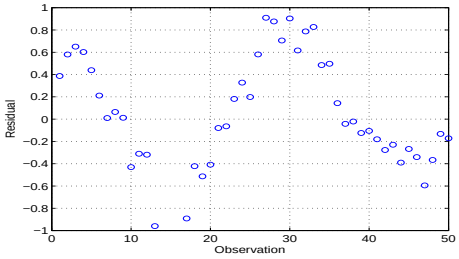

3.5.2: Second Order RSM

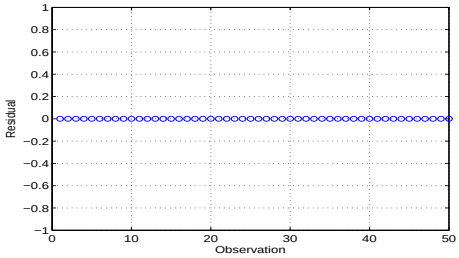

3.5.3: RBF

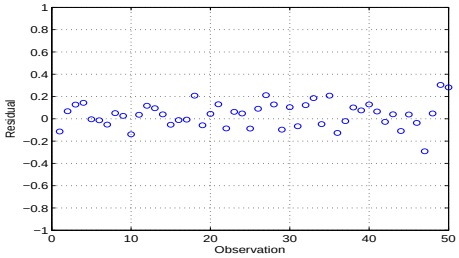

3.5.4: Kriging

Figure 3.5: Residual Plots for $y = 2\sqrt{x} + \cos(x) + \epsilon$

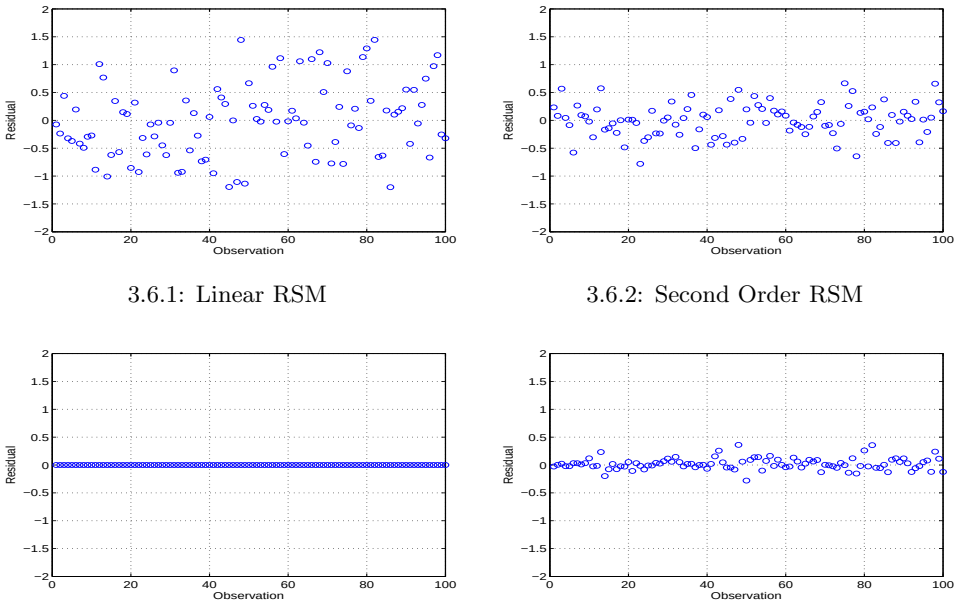

3.6.1: Linear RSM

3.6.2: Second Order RSM

3.6.3: RBF

3.6.4: Kriging

Figure 3.6: Residual Plots for $y = \sqrt{x_1} + \sqrt{x_2} + \cos(x_1) + \cos(x_2) + \epsilon$

3.4 Kriging Hyperparameter Strategy

Kriging is unique in that there are undetermined parameters that affect the fit of the metamodel that the user can choose. This can be viewed as a weakness of the kriging process because RBF/RSM are truly determined by the data. It is a best practice to choose these hyperparameters in a way that minimizes the error between the predicted mean value and the observed mean value. This can be accomplished using an iterative cross-validation method letting the hyperparameters float until the minimum error is achieved. However, this adds a one-time fitting penalty to the kriging process. Subsequent metamodel evaluations do not require re-optimizing the hyperparameters for the same set of observed data.

Chapter 4

Combustion and Autoignition

4.1 Introduction

Combustion is perhaps the most prevalent form of energy conversion in the world today. Combustion releases energy stored in fuel in the form of heat which is then used in a thermodynamic cycle to do work. This work can turn a generator for electricity or a crankshaft in a car. Combustion typically requires three elements to be present for the exothermic reaction to occur: fuel, oxidizer, and a source of ignition. For example, in an Otto cycle automotive engine, the fuel is gasoline (a hydrocarbon), the oxidizer is air, and the ignition source is the spark plug. Under certain conditions, the fuel and oxidizer may combine and spontaneously ignite in a phenomenon called autoignition. In Otto cycle (constant volume combustion) automotive engines, this is referred to as "knock" [2] and is avoided due to the adverse mechanical consequences of such a rapid, unintended pressure rise. Diesel cycle engines (constant pressure combustion), however, use autoignition as the method to initiate the combustion process and drive the power stroke of the cylinder. Furthermore, the Brayton cycle (applied to gas turbines for power generation and propulsion) is also constant pressure combustion but the process is open, meaning mass (fuel plus air) is not conserved but *mass flow rate* is conserved. Brayton cycle combustion is initiated by a spark but sustained by the existing combustion flame with the fuel and oxidizer being constantly replenished and a stationary flame front. Autoignition in the Brayton cycle can be defined as a rapid heat release without a source such as a spark or existing flame front[6]. This negatively impacts combustor hardware and emissions.

Autoignition phenomena in through flow combustion systems, such as those found in

gas turbines, is described through a chemical delay time of the fuel and oxidizer mixture. This delay time is modeled using single step reaction theory from the field of chemical kinetics [7]. This simplification of the complex chemical processes that govern combustion is practical but is not accurate enough for finding and quantifying a true autoignition boundary for a particular hardware design. Commercial simulation software (CHEMKIN, etc) exist to model these types of chemical reactions but certain simplifying assumptions must be made regarding the hardware configuration to integrate into the software. Lastly, experimental autoignition ignition delay time investigations involve the use of idealized shock tube hardware with surrogate fuel and oxidizer properties (pressure, temperature, etc) that are not necessarily reflective of a Brayton cycle combustion system [24].

The combination of the above factors (simple, physics based equations, higher fidelity computer model, and physical experiment data) make autoignition phenomena an ideal candidate for system level optimization. Additionally, the combination of chemical kinetics and physical flow properties also make autoignition an excellent candidate for meta-modeling since there is no single unified software package to calculate chemical kinetics and fluid flow properties. Deterministic optimization methods can produce an ideal design that minimizes autoignition risk. But, due to the rarity of this event in a production level hardware design and severe safety consequences of an event (if applied to aircraft engine gas turbines), stochastic methods should be used to quantify the risk of occurrence and feedback to the hardware design cycle ways to minimize this risk. Furthermore, todays manufacturing capability cannot economically produce the ideal hardware design intent for every single part coming off of the production line. There exists inherent variability due to manufacturing tolerances that influence a system's risk of autoignition.

The focus of this work is developing the deterministic and stochastic methods to optimize a design for autoignition risk. To maintain scope, a simplified hardware model is used to demonstrate model building and optimization techniques. In practical application, the high fidelity computer simulations and experimental data can be generated with complex (and often proprietary) hardware found in a modern combustion system.

4.2 Physics of Autoignition

In a continuous flow combustion system, fuel is injected into an air stream ahead of the flame front. This allows the fuel and air to mix adequately before ignition due to the existing flame. During this mixing process, complex chemical reactions are occurring. Those reactions and the rate at which they occur fall under the broad scope of chemical kinetics which is outside the scope of this work. A simplifying assumption can be made that allows the complex mixing/igniton/combustion process to be described with a single step global reaction mechanism. Higher fidelity analysis with specialized software (ie. CHEMKIN) can capture multistep reaction detail. The formation of combustion products from fuel and air in a single step is described by Equation 4.1 [21]:

$$F + Ox \rightarrow Prod \tag{4.1}$$

The reaction proceeds at the rate:

$$\frac{d\left[F\right]}{dt} = -k\left[F\right]\left[Ox\right] \tag{4.2}$$

where k is called the rate coefficient[21]. The rate coefficient can be derived through molecular collision theory and can be summarized in the Arrhenius form:

$$k = A\exp\left(\frac{-E_a}{R_u T}\right) \tag{4.3}$$

where A is called the pre-exponential factor, E_a is the activation energy of the fuel, R_u is the universal gas constant, and T is the temperature of the fuel-air mixture[21]. Because of the empirical nature of the pre-exponential factor, it can contain a units conversion to allow the rate coefficient to have units of time. This is described as the chemical ignition delay time (t_{chem}) [6]. The pre-exponential factor also has a strong dependency on pressure

and fuel stoichiometry (ϕ) so the ignition delay can be broken down into:

$$t_{chem} = AP^m \phi^n \exp\left(\frac{E_a}{R_u T}\right) \tag{4.4}$$

Now, A, m, and n must be determined experimentally [6]. This form is commonly used in experiment setups plotted against 1/T [7, 8, 24, 20]. In the absence of an external ignition source, the fuel-air mixture with activation energy E_a, empirical coefficients A, m, and n, and at pressure P and temperature T will spontaneously ignite after time t_{chem}. For simplicity in demonstration, empirical factors and activation energy are used as recommended by Lefebvre [7] and summarized in Table 4.1.

Parameter	**Value**	**Description**
E_a	1.236×10^{-3}	Activation Energy
A	60×10^{-3}	Pre-exponential Factor
R_u	1.986	Universal Gas Constant
m	0.98	Pressure Exponent
n	0.37	Stoichiometry Exponent

Table 4.1: Assumed Autoignition Empirical Parameters (based on Lefebvre [7])

To avoid autoignition, the fuel-air mixture must meet a source of ignition *before* the ignition delay time t_{chem}. The time that the unburnt fuel-air mixture spends residing in the combustion apparatus can be calculated using CFD or with some simplifying assumptions on the hardware. At the lowest fidelity, the flow residence time is a length over a velocity,

$$t_{res} = \frac{L_{phys} c_L}{V} \tag{4.5}$$

where the length is the distance traveled by the unburnt fuel-air mixture between fuel introduction and burning. There is some abstraction to this length because fuel atomization and droplet evaporation effects distort the true, physical length between the fuel introduction plane and the flame front. For complex combustion geometry, the true length is corrected

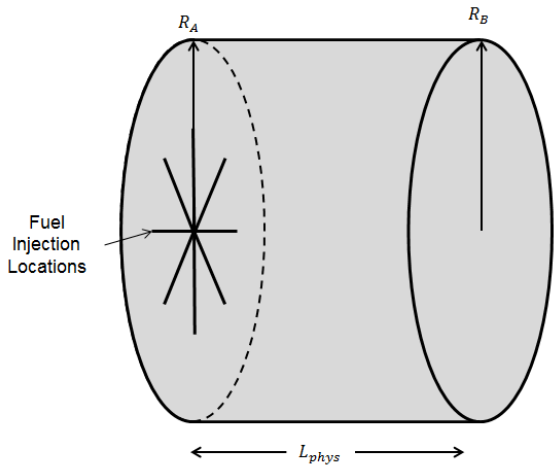

Figure 4.1: *Simplified Reactor Geometry*

by a factor derived from CFD or other experiment to accommodate non-cylindrical features. For the sake of simplicity, this work assumes an uncorrected cylindrical length ($c_L = 1$) and assumes the flame is stable on the trailing edge of the device. The velocity in Equation 4.5 is the average velocity of a particle of the fuel-air mixture across the length.

In the absence of production level combustor hardware, a simplified mixing chamber model will be used to demonstrate the flow time principles. The simplified hardware is shown in Figure 4.1. The designer has control over L_{phys}, R_A, and R_B. To enhance mixing, the designer may opt to control the inlet flow so as to swirl it through the reactor. The designer may also choose to contour the outer wall as shown in Figure 4.2. Due to manufacturing tolerances, this wall contouring may exist in a production part without design intent. Swirl and wall contouring may be accommodated by adjusting the length coefficient. The production part may also show elliptical deformation as shown in Figure 4.3. In addition, there are inevitable manufacturing tolerances on the radii and length of the reactor. This variation is input into a Monte Carlo analysis to quantify its impact. It is the intent of robust design to optimize these hardware tuning knobs (length, radius) to minimize risk of autoignition.

The final element in the chemical time (t_{chem}) is related to fuel stoichiometry, or fuel-air

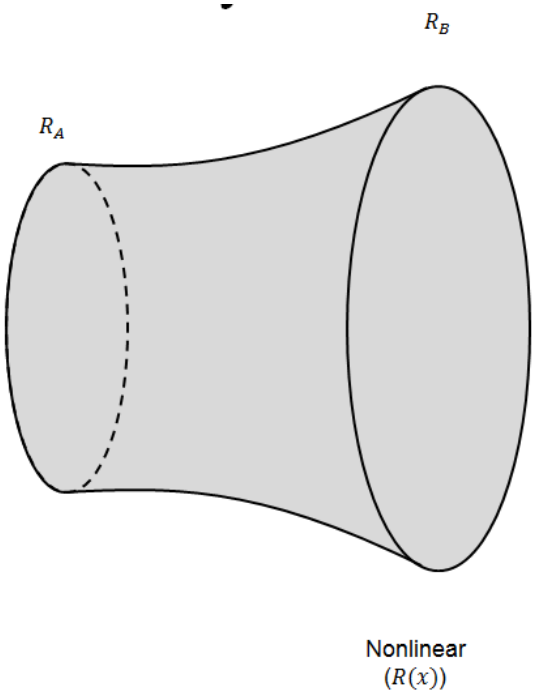

Figure 4.2: *Simplified Reactor Contoured Wall*

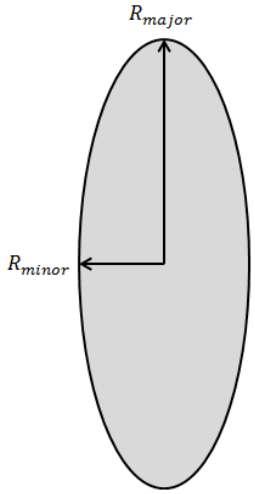

Figure 4.3: *Simplified Reactor Elliptical Deformation (exaggerated)*

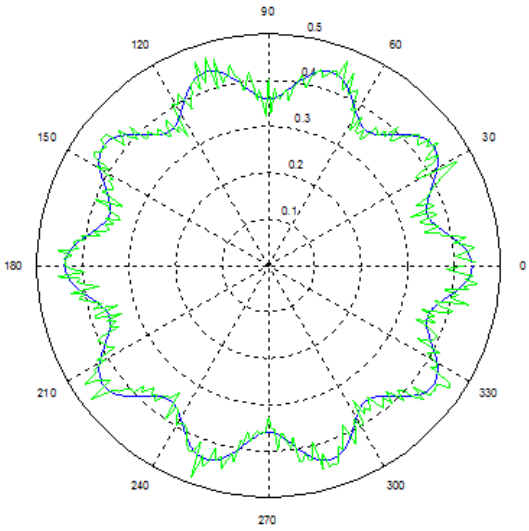

Figure 4.4: *Fuel Stoichiometry Variation*

ratio. The ratio of true fuel-air ratio to the stoichiometric fuel-air ratio is ϕ. For $\phi < 1$ the mixture is lean meaning excess air is available for combustion. Conversely, $\phi > 1$ classifies a rich mixture. This analysis assumes $\phi = 0.4$ as recommended by Lefebvre [6] as a representative value for modern lean burn gas turbine combustors. An extension of this work can analyze local three dimensional variation in ϕ around the fuel injection locations. This is left for future work because of the low chemical time dependency on ϕ (exponent $n = 0.38$). Local ϕ variation is depicted graphically in Figure 4.4.

Finally, the flow time and ignition delay time can be related through the simple ratio

$$Da = \frac{t_{res}}{t_{chem}} \tag{4.6}$$

where Da is known as the Damkohler Number [21]. It follows that for $Da \geq 1$, autoignition will occur within the effective flow length established above. Conversely, if $Da < 1$, autoignition will not occur.

Chapter 5

Autoignition Metamodeling

5.1 Physics based functional form

From the previous chapter, the functional form of the Damkohler autoignition predictor is

$$Da = \frac{t_{res}}{t_{chem}} = \frac{L/V}{AP^m \phi^n \exp\left(\frac{E_a}{R_u T}\right)} \tag{5.1}$$

where bulk flow velocity (V) is inversely proportional to flow area

$$V = \frac{W_{in}}{\rho \cdot Area} \tag{5.2}$$

and area (A) is the cylindrical cross section.

$$Area = \pi Radius^2 \tag{5.3}$$

Departures from cylindricity such as coning, wall contouring, or elliptical deformation can be handled by the length coefficient (c_L) adjustment derived from CFD or other higher fidelity analysis. For simplicity, this work assumes perfect cylindricity with variation on radius.

In practical combustion design problems, the incoming flow properties (P_{in}, T_{in}, W_{in}, ϕ) are typically set by higher level system requirements such as gas turbine cycle performance. The chemical constants (A, m, n, E_a) and physical flow properties (R_u, ρ) are known or assumed based on previous work or literature. This leaves the designer influence over combustion hardware (*radius*, *length*). For simplicity, a design space consisting only of

device radius and length are considered. Explorations of plus and minus 25 percent around an assumed nominal length and plus and minus 20 percent around an assumed nominal radius is assumed to be adequate. See Figure 6.4 for a graphical representation of the assumed design space and current hardware variation limits.

As shown in Figure 5.1.1, Damkohler number and thus autoignition risk minimize in the lower left quadrant. This corresponds to a -25% radius and a -20% mixing length. However, in real combustion systems, autoignition is never the only critical parameter. The overall system must be balanced in terms of combustion efficiency and autoignition (among others).

5.2 Multiobjective Desirability Function

Combustion efficiency is a measure of how much energy (heat) is released compared to how much energy is available in the fuel. This heat release is a function of chemical kinetics, flame velocity, air-fuel mixing, and fuel evaporation. Calculation of an absolute level of combustion efficiency requires detailed analysis of each of these elements and is out of the scope of this work. However, *relative* combustion efficiency is often correlated as a function of combustion operating conditions such as pressure, temperature, mass flow rate, and combustor dimensions [6]. For an optimization effort on an existing design, relative efficiency is most important to the designer in determining if one combination of independent variables is better/worse than another. This relative combustion efficiency is the maximization objective for this simplified autoignition study and is modeled according to Lefebvre's recommendation [6] :

$$\eta_{comb} \propto f\left(W_{in}\right)^{-1}\left(\frac{1}{t_{res}\left(P_{in},T_{in},Len,Radius\right)}+\frac{1}{t_{chem}\left(P_{in},T_{in}\right)}\right)^{-1} \tag{5.4}$$

As shown in Figure 5.1, efficiency maximizes in the upper right quadrant and Damkohler minimizes in the lower left quadrant. To optimize this system for these responses, a desirability function approach is used as outlined in Meyers and Montgomery inspired by Derringer and Suich [14]. The desirability function is

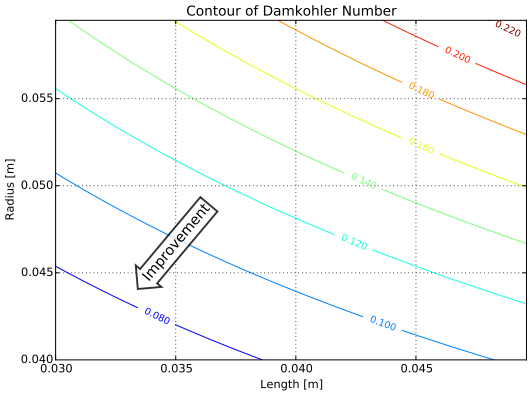

5.1.1: Contours of Damkohler number

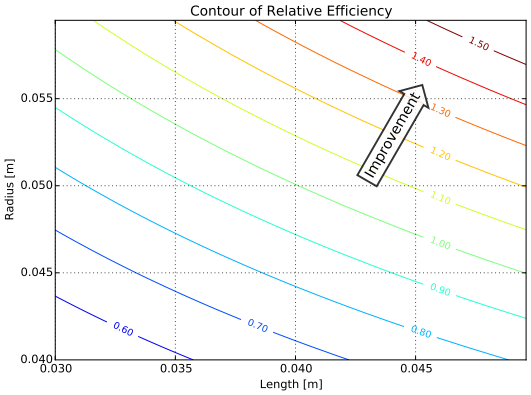

5.1.2: Contours proportional to efficiency

Figure 5.1: Damkohler and Efficiency for the assumed design space

$$D = (d_1 d_2 \dots d_m)^{\frac{1}{m}} \tag{5.5}$$

where each component varies between zero and one according to some simple rules. If the target T is a maxima of the response y and L is a lower bound,

$$d = \begin{cases} 0 & \text{when } y < L \\ \left(\dfrac{y-L}{T-L}\right)^r & \text{when } L \le y \le T \\ 1 & \text{when } y > T \end{cases} \tag{5.6}$$

If the target T is a minima of the response y and U is an upper bound,

$$d = \begin{cases} 0 & \text{when } y < T \\ \left(\dfrac{U-y}{U-T}\right)^r & \text{when } T \le y \le U \\ 1 & \text{when } y > U \end{cases} \tag{5.7}$$

Generally, if the target T is located between an upper and lower bound,

$$d = \begin{cases} 0 & \text{when } y < L \\ \left(\dfrac{y-L}{T-L}\right)^{r_1} & \text{when } L \le y \le T \\ \left(\dfrac{U-y}{U-T}\right)^{r_2} & \text{when } T \le y \le U \\ 0 & \text{when } y > U \end{cases} \tag{5.8}$$

where the r factors are weights determined by the user. For this deterministic optimization example, the r values are unity giving autoignition and efficiency equal weight. This overall desirability method is simple and effective in turning a complex multiobjective optimization problem into a single objective function that can be operated on for any optimization algorithm. This approach is expandable to any number of objectives which is critical for system level design optimization.

Figure 5.2 shows the desirability contour for the multiobjective design optimization problem to maximize combustion efficiency and minimize tendency to autoignite. The result shows a locus of maximum desirability from the top left quadrant to the lower right quadrant.

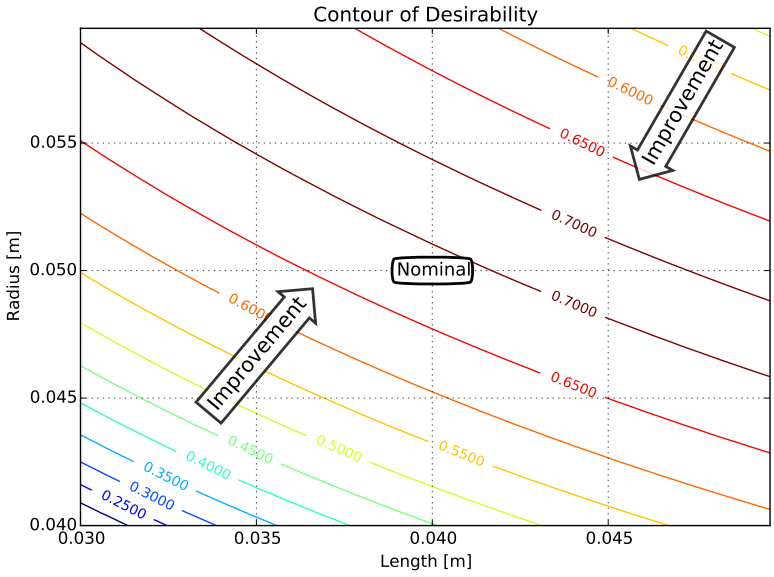

Figure 5.2: Contours of desirability for a ±10% design space

5.3 Design of Experiments and Metamodeling

Now that the physics of the system are established and the optimization objectives of autoignition and efficiency are defined, the design and experimentation process can be emulated with an assumed level of observation noise or process variability. Accounting for noise in this first step is essential to tracking variance of the critical system output characteristics (efficiency, autoignition) and establishes the foundations for a robust design.

For metamodel fitting of observed data, the designer must deal with variance in dependent parameters (in the form of observation uncertainty) in addition to allowed tolerance variation in independent parameters. This variance is quantified by repeating an experiment for the exact same settings of independent parameters and observing the output. In practical design problems, the engineer is given an experiment budget and must obtain the most information about a system without exceeding the budget. Part of this budget is also dedicated to validating the optimal independent parameters and quantifying the expected variability during production. Validation experiments may also be used to prove adequate margin to a design requirement. This is especially relevant to the combustion autoignition problem since the system must comply with an appropriately low instance of occurrence during operation.

For this level of analysis of the combustion autoignition problem, the observable time characteristics (t_{chem}, t_{res}) and geometric features (length, radius) for the above physics are assumed to have a two sigma variance of $\pm 10\%$. This assumption can be further refined as data is gathered on the process. Future work can increase fidelity on sensitivity by removing the assumed bulk time variation and including variation specific to physics based parameters such as fuel properties (activation energy E_a, pre-exponential factor A, pressure and stoichiometry exponents m,n) and geometric properties (wall contouring, flow swirl).

5.3.1 Traditional DoE

Traditional Design of Experiment theory is geared toward first or second order deterministic response surface metamodeling. Identifying a direction of improvement is the major result (as opposed to finding the global optima in the design space) in traditional DoE theory.

First Order RSM

From 2.2.2, a first order response surface model is built using regression coefficients to minimize the error in the linear model predicted value from the observed value. The variance of these regression coefficients are minimized by the unique class of orthogonal first-order experiment designs [13]. The most common of this class is the 2^k series of designs. This series is made up of two levels for each of k independent variables. A schematic of a 2^2 and 2^3 designs are in Figure 5.5. The main drawback of the 2^k series of designs is that no estimate of experiment variance can be made without replication of design points. Since 2^k designs are sufficient for linear models, the applicability to complex non-linear problems is very limited.

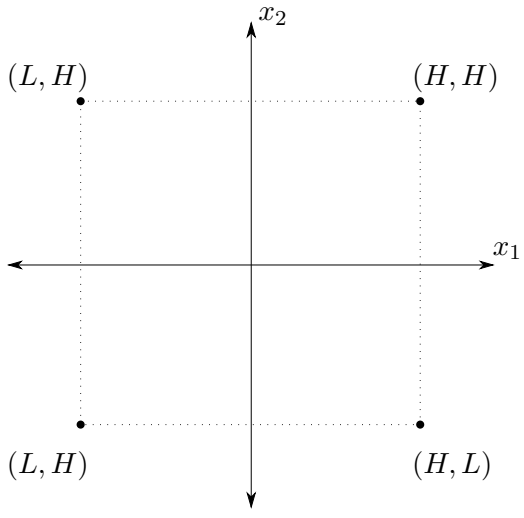

5.3.1: 2^2 Design Schematic

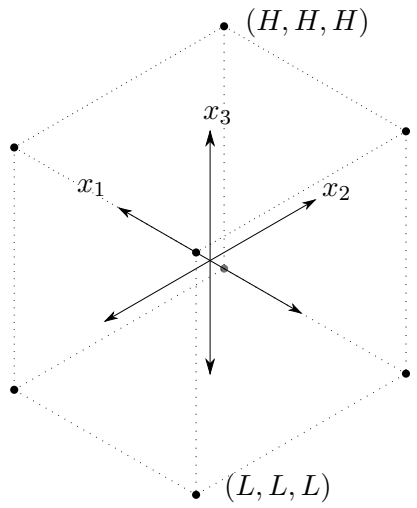

5.3.2: 2^3 Design Schematic (some labels omitted for clarity)

Figure 5.3: General 2^k Traditional DoE Experiment Designs

To set up a real-world design scenario, whose objective is to optimize the combustion

system, using a 2^k experiment design, the user must designate a "low" and "high" level of the independent variables. Using the physics-based desirability function plotted in Figure 5.2, the low-high value pair will be $\pm 6\%$ for the length and radius independent variables. As a surrogate for physical experiment data, noise will be added to the physics-based model for use as "observed" data points. Recall, the true underlying desirability contour is unknown to the designer at this point. The objective is to re-target the system on the locus of maximum desirability.

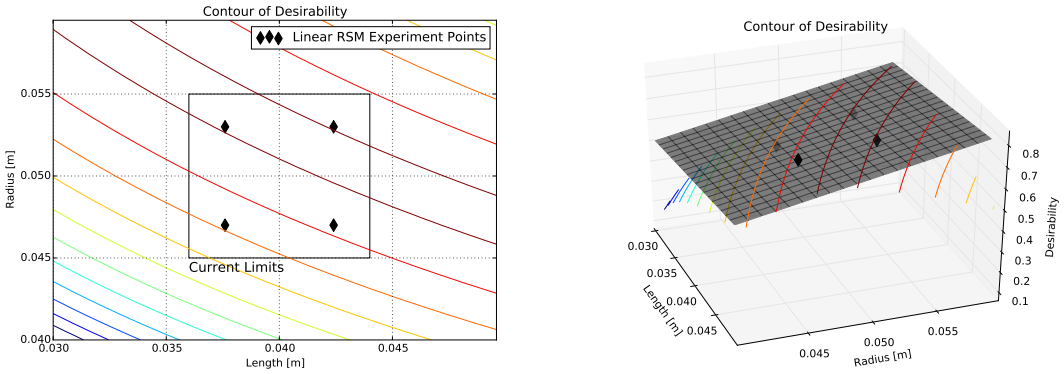

5.4.1: Combustion 2^2 design

5.4.2: Resulting Linear RSM for 2^2 design

Figure 5.4: Combustion Optimization 2^2 DoE

The linear surface through the (simulated) noisy desirability observations is plotted in Figure 5.4.2 using the linear RSM procedure outlined in Section 2.2.2. The direction of improvement is identified but overshoots the locus of maximum desirability. A higher order response surface model may be more appropriate.

Second Order RSM

According to Meyers and Montgomery [14], a second order response surface metamodel requires the following minimum conditions:

1. More than three levels of each design variable.
2. More than $1 + 2k + k(k-1)/2$ distinct design points where k is the number of independent parameters.

A Central Composite Design (CCD) is the most popular design for fitting second order RS models [13]. The CCD is composed of additional axial experiments on top of the general 2^k design and a central experiment at the nominal value. The center point is often repeated to determine variance. According to Box and Hunter [1], rotability is an important characteristic in second order RS experiment designs. Rotable designs provide information at symmetrical distances around the nominal, that is, circles or spheres around the nominal. CCD experiments satisfy this recommendation.

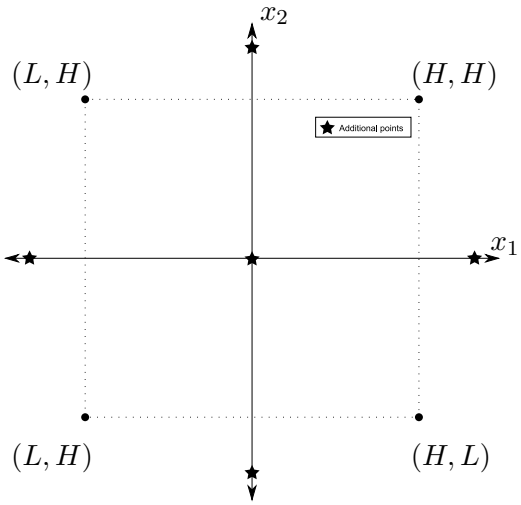

5.5.1: 2 Factor Schematic

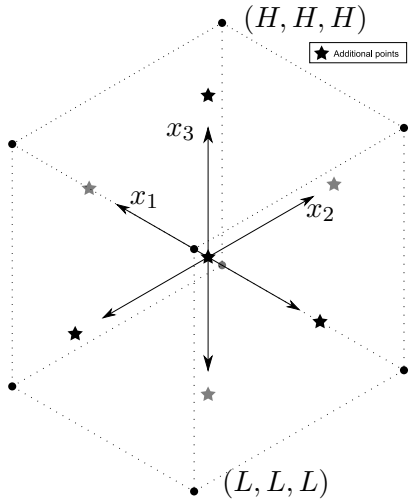

5.5.2: 3 Factor Schematic

Figure 5.5: Cetral Composite Designs

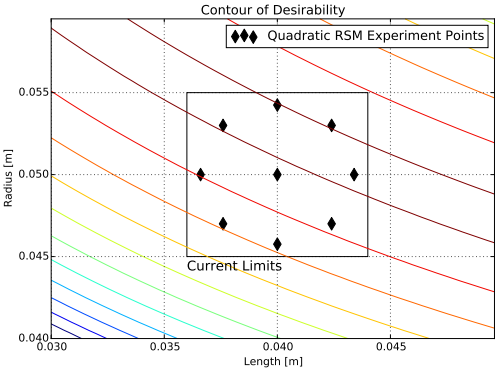

5.6.1: Combustion CCD design

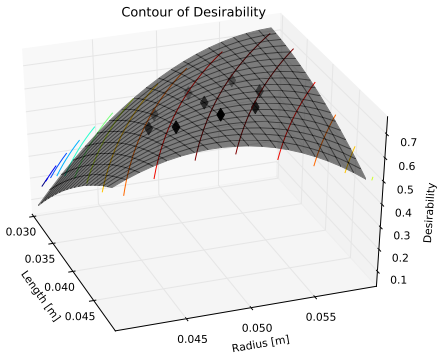

5.6.2: Resulting Quadratic RSM for CCD design

Figure 5.6: Combustion Optimization CCD DoE

The second order desirability response surface is plotted in Figure 5.6.2 based on the simulated noisy experiment observations at locations identified in Figure 5.6.1 following a Central Composite Design.

Traditional DoE methods such as 2^k for linear RSM or CCD for higher order RSMs are ineffective if used singly since only direction of improvement (linear RSM) or curvature (higher order RSM) information can be obtained through traditional experiment designs. An efficient design process uses linear models to screen the design space and approach the optimal design iteratively using sequential experimentation and model fitting with increasing levels of fidelity. Another efficient method to find the global optima of a system is the use of modern DoE methods to build a non-RS metamodel of the system.

5.3.2 Modern DoE

Where traditional DoE methods mainly serve to improve an existing design, modern DoE methods aim to explore a wide design space. These modern designs are especially useful for computer experiments (CFD) because they evenly distribute sampling points throughout design space [14]. These space filling designs typically do not contain repeated experiments since variance can be estimated from the whole sampled population. Examples of space-filling designs are Latin hypercube, sphere packing, uniform, and maximum entropy.

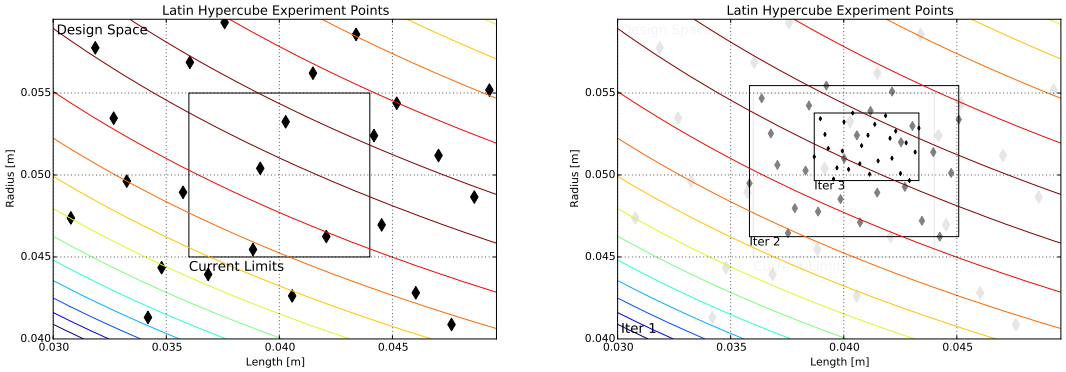

5.7.1: Optimal Latin Hypercube Sampling

5.7.2: Sequential Design Space Narrowing

Figure 5.7: Modern DoE Sampling Methods

Modern DoE methods are more suitable to advanced metamodeling techniques like kriging and provide more information about the response for a more robust metamodel. Modern DoE techniques assume that metamodels accurately predict the response within a known uncertainty. This approach allows the designer to take a broad view of the entire design space and sequentially "zoom in" on an optimal region. This ensures the designer doesn't erroneously choose a local optima because of a poor choice in step size during sequential experiment rounds. The zooming is best described as experimenting at a very coarse resolution but covering the entire design space then iteratively narrowing the design space centered on the optima of the previous round and increasing the experiment resolution. The most efficient experiment plan will leverage a combination of the above traditional and modern DoE techniques.

Chapter 6

Autoignition Stochastic Considerations

Probability is the likelihood of occurrence of an event with random variation. These occurrences can be distributed many different ways, the simplest of which is where all outcomes have an equal chance of occurrence. These events are characterized as uniformly distributed. In industry, many manufacturing processes produce parts that are most likely to occur in the middle or mean of their drawing limits with some acceptable band to accommodate inherent variation. This is a common example of the Gaussian or Normal distribution. This work focuses primarily on the extrema of a probability distribution where events are least likely to occur, also known as rare events.

Autoignition by nature is a rare event. Difficulties in observing autoignition create challenges for assessing risk and guiding design. Furthermore, the probability of an autoignition event may be constrained to fall below a minimum acceptable probability. Since autoignition may be viewed as a safety hazard in some applications, this acceptable event probability is vanishingly small (10^{-9} as noted previously). The probability of autoignition, $P(A)$, can be described as the expected value of an indicator variable, $h(x)$. It is established that Damkohler number is the proper variable where a value greater than one is an indicator of autoignition. Autoignition will not occur for Damkohler less than one.

$$P(A) = E\left[h(\mathbf{x})\right] = \int_{-\infty}^{\infty} h(x) f(x) dx \tag{6.1}$$

where $f(x)$ is the probability density function of the input variables $\mathbf{x}$ and $h(\mathbf{x})$ is the indicator function.

$$h(\mathbf{x}) = \begin{cases} 0 & \text{when } Da < 1 \\ 1 & \text{when } Da \geq 1 \end{cases} \tag{6.2}$$

The traditional way to calculate the expectation of the indicator is to simply take its mean.

$$E\left[h(\mathbf{x})\right] = \mu_h = \frac{1}{n}\sum_{i=1}^{n} h(x_i) \tag{6.3}$$

The 95% confidence around this expectation is given by

$$CI_{0.95} = \mu_h \pm 1.96\frac{\sigma_h}{\sqrt{n}} \tag{6.4}$$

where σ is the standard deviation of the indicator variable and n is the number of samples.

6.1 Statistical Environment Profile

Until now, the problem has been formulated with only two independent variables (length and radius). However, in revisiting the autoignition physics equations in Section 5.1, it is apparent that operating conditions (pressure and temperature) play a significant role in the predictor of autoignition. These variables are considered uncontrollable from a hardware designer's perspective because, in gas turbine applications, the operating conditions are governed by the overall needs of the thermodynamic cycle. In extreme situations, the hardware designers must iterate with the cycle designers to impose cycle limits where the risk of autoignition is unacceptable. For the deterministic optimization problem, these uncontrollable cycle values were assumed to be fixed at a level that seeded the problem heavily toward autoignition. In normal operation, the combustion system rarely experiences these severe conditions so the true autoignition tendency measured over the entire operating regime is less than that which was represented during deterministic optimization. This method of purposely selecting low-occurrence independent variables to increase

the severity of the system is a form of indirect importance sampling. In fact, this sort of indirect importance sampling is common in industrial reliability testing in the form of accelerated life consumption methods. During these tests, in a very short time, the system is exposed to extreme conditions that rarely occur during normal operation. Successful completion of accelerated life testing at the factory is often a product requirement before it can be released to the field and customers.

To understand the variation in operating conditions, a representative commercial aircraft mission is presented in Figure 6.1.

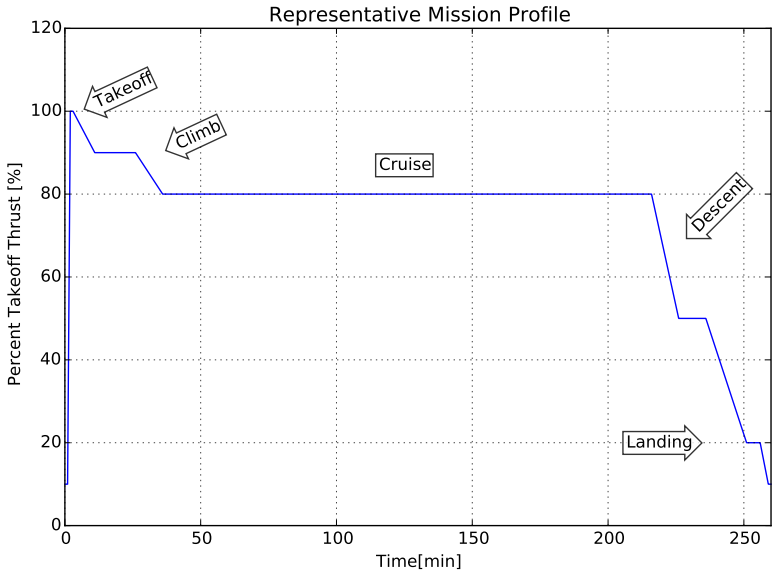

Figure 6.1: Representative Mission

Pressure and temperature data for points in the above mission were generated using the Elements of Propulsion PERF program by Mattingly [9] assuming a simplified single spool turbojet model. Generated design data is found in Table 6.1. These combustion environment conditions are plotted for the entire mission in Figure 6.2. Mass flow is heavily correlated with pressure and temperature and does not contribute significantly to system variation as an independent parameter. For simplification, mass flow is considered a pure function of pressure and temperature, leaving these as the two selected stochastic

	% Takeoff Thrust	Altitude [ft]	Mach No.	P [atm]	T [K]	Wtot [kg/s]
Taxi	10	0	0	5.78	512.7	29.0
Takeoff	100	0	0.2	27.70	832.2	91.6
Climb	90	10000	0.5	20.62	791.6	70.3
Cruise	80	35000	0.8	8.30	675.0	30.8
Descent	50	10000	0.5	13.34	692.7	50.3
Landing	20	1000	0.2	8.71	585.5	38.6
Taxi	10	0	0	5.78	512.7	29.0

Table 6.1: Combustion Environment Conditions throughout Representative Mission

independent variables.

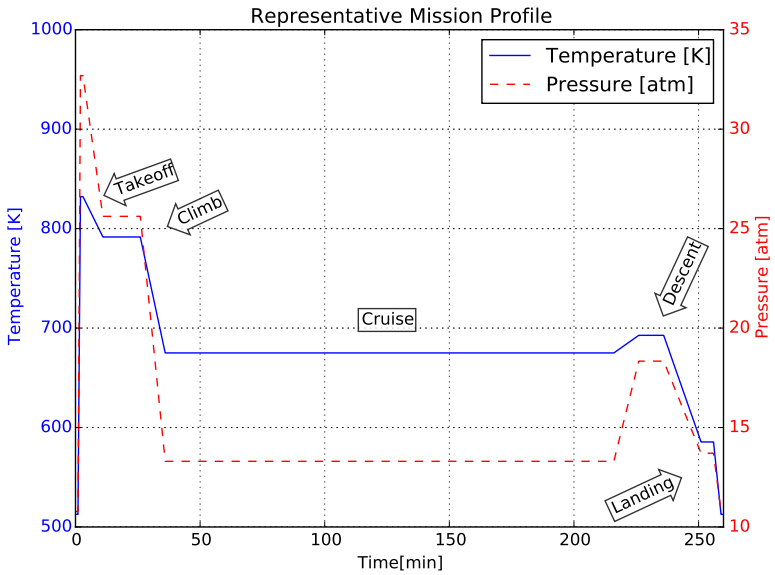

Figure 6.2: Pressure and Temperature Profile for the Representative Mission

The mission can be discretized into autoignition "opportunities" for probabilistic evaluation. For simplicity, the discretization will occur in 0.1 sec increments. This is a good assumption since 0.1 sec is on the order of 500x the combustion chemical time scale ($\sim 0.2ms$). After discretization, the pressure and temperature opportunities can be fit to a multivariate

	Mean	Covariance	
Temperature	683.2 K	2290.6	171.8
Pressure	15.27 atm	171.8	18.5

Table 6.2: Resulting Fit Parameters for Discretized Mission Data

normal distribution (Table 6.2 and Figure 6.3). This discretization process also enables an uncertainty quantification on the autoignition predictor (Damkohler number) for a fixed hardware design (length and radius are known and constant).

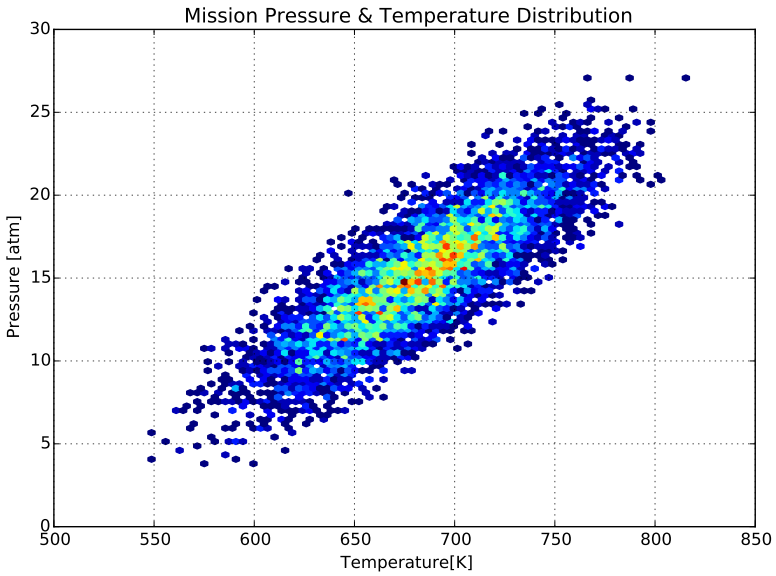

Figure 6.3: Pressure and Temperature Density for Representative Mission

6.2 Monte Carlo Analysis

For practical systems, the optimal target setting for an independent parameter will not be produced for every single part. A balance must always be struck between manufacturability and performance. There is a strong correlation between manufacturing cost and geometric tolerance (lower cost implies larger tolerance) so by driving cost down, product variability will increase. In designing a new part, the engineer must choose an appropriate tolerance to balance performance and cost. Monte Carlo methods are traditionally used to evaluate the

performance and variability of a system due to manufacturing tolerances. The tolerances on radius and length are modeled as independent truncated normal distributions with an assumed two sigma variance of ±10%.

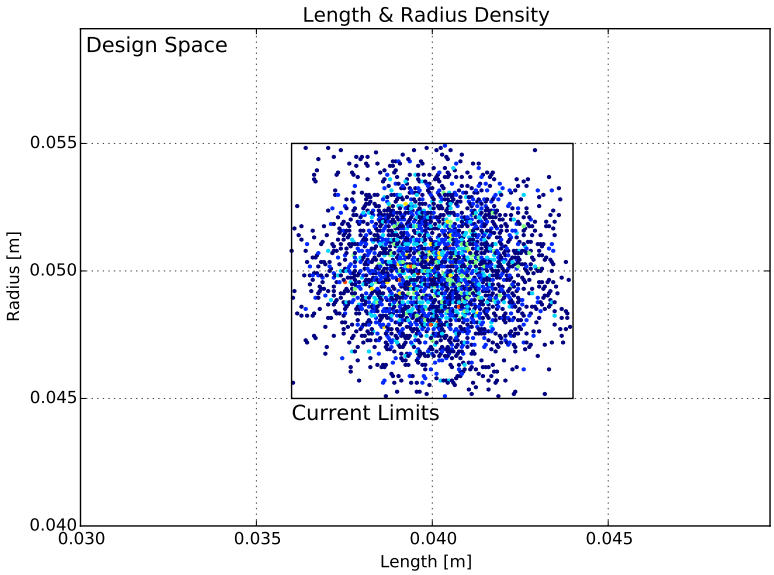

Figure 6.4: Assumed Length And Radius Density Distribution

Now that the distributions are known for the controlled (length, radius) and uncontrolled (pressure, temperature) independent variables, Response Surface Methodology can be applied with stochastic adaptations to address model uncertainty. This non-deterministic branch is formally known as Robust Design Simulation (RDS) [10, 11] and takes into account mean and variance of a response during optimization. To facilitate variability accommodation in the design process, Mavris' [10] RDS methodology uses Monte Carlo methods to quantify the distribution on the output of the response surface model. This response surface model is generated using traditional DoE techniques. Mavris shows that Monte Carlo analysis is an effective tool to extract probabilistic information from a deterministic model.

For this application, the RDS methodology would be implemented using metamodels developed in Section 5.3.1. These metamodels would be evaluated efficiently using Monte

Carlo sampling on the independent parameters (length, radius, pressure, and temperature) to build a distribution on the response (system desirability function). The goal of RDS is to influence the mean and variance of controllable independent parameters (such as a drawing tolerance) to minimize sensitivity to variation in the response. Another outcome of this Monte Carlo RDS approach is a probability assessment of autoignition risk for a given setting on controllable independent parameters and a given mission. This risk is evaluated using the Damkohler metamodel and must be below a certain threshold to be considered safe. For this analysis, probability of autoignition occurrence less than 10^{-9} is acceptable. Recall, an autoignition occurrence is defined as a Damkohler number greater than one. Autoignition is characterized as a rare event.

6.2.1 Importance Sampling Theory

For the engineer using traditional Monte Carlo methods to simply observe one rare event with a 10^{-9} probability, 999,999,999 successful observations must also be made. This can get prohibitively expensive to evaluate, even with a metamodel. In addition, to extract any variance estimate for this rare event, many more simulations must be run. To achieve 95% confidence in estimating a 10^{-9} event, the simulation sample size must be larger than 3.84×10^{11} [18]. (See Appendix B.2 for derivation.) To reduce this requirement for such a huge sample population (many samples of which are irrelevant to the rare event), importance sampling is used as a method to increase observances of the rare event by sampling only at relevant locations.

Importance sampling is a statistical technique to artificially increase the likelihood of encountering a rare event by sampling from an alternative density function represented here as $g(\mathbf{x})$.

$$P(A) = \int_{-\infty}^{\infty} h(x)\frac{f(x)}{g(x)}g(x)dx = E_g\left[\frac{h(\mathbf{x})f(\mathbf{x})}{g(\mathbf{x})}\right] \tag{6.5}$$

This alternative density function is chosen by the user as a region where the rare behavior is very likely to occur. For the autoignition problem, an increase in pressure and a decrease in temperature will drive autoignition tendency higher. This mean shifted

density function is shown in Figure 6.5.

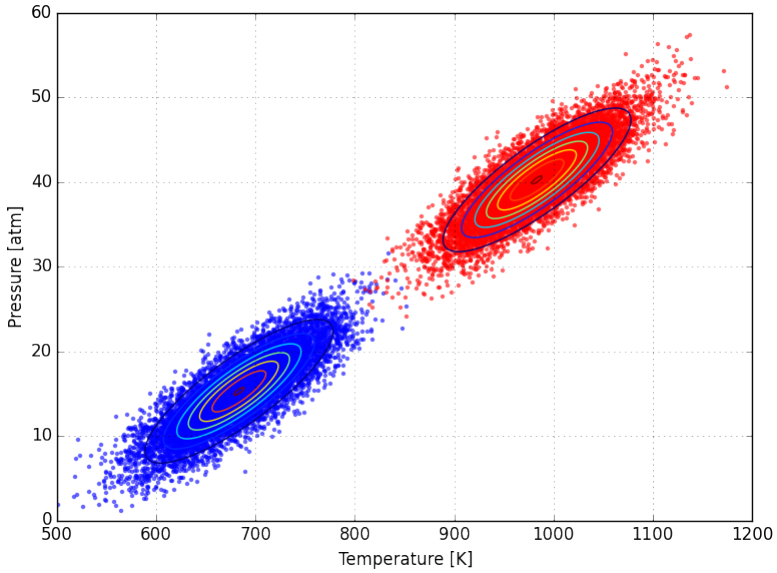

Figure 6.5: Mean Shifted versus Original Distributions on Pressure and Temperature

The probability of autoignition is now the expectation of the indicator variable ($h(\mathbf{x})$) multiplied by the ratio of the original ($f(\mathbf{x})$) and modified ($g(\mathbf{x})$) density functions. This ratio is called the *likelihood ratio*.

The distributions on environment conditions (pressure, temperature) lend themselves toward importance sampling since extreme conditions that favor autoignition occur rarely during the operational life of a combustion system. The pressure and temperature expected during normal operation were characterized by a bivariate normal probability density (Table 6.2 and Figure 6.3). The bivariate normal probability density function is given by [17]:

$$f(x,y) = \frac{1}{2\pi\sigma_x\sigma_y\sqrt{1-\rho^2}} e^{-\frac{1}{2(1-\rho^2)}\left[\left(\frac{x-\mu_{xf}}{\sigma_x}\right)^2+\left(\frac{y-\mu_{yf}}{\sigma_y}\right)^2-\frac{-2\rho}{\sigma_x\sigma_y}(x-\mu_{xf})(y-\mu_{yf})\right]} \tag{6.6}$$

where (x,y) is the point at which the sample is taken, μ_{xf} is the mean value of x, μ_{yf} is the mean value of y, σ_x and σ_y are the standard deviations of the x and y random variables, and ρ is the correlation coefficient found in the off-diagonal of the covariance matrix. The

	Original f	**Shifted** g	**Delta**
μ_x	683.2	983.2	300
μ_y	58.3	83.3	25
σ_x	$\sqrt{2290.6}$	$\sqrt{2290.6}$	
σ_y	$\sqrt{18.5}$	$\sqrt{18.5}$	
ρ	$\frac{171.8}{\sigma_x\sigma_y}$	$\frac{171.8}{\sigma_x\sigma_y}$	

Table 6.3: Multivariate Normal Distribution Parameters

f subscript indicates the original density.

To find the likelihood ratio (LR) for this importance sampling problem, the original multivariate probability density function will be compared to a mean-shifted probability density function (subscript g) with the same covariance matrix [23].

$$g(x,y) = \frac{1}{2\pi\sigma_x\sigma_y\sqrt{1-\rho^2}} e^{-\frac{1}{2(1-\rho^2)}\left[\left(\frac{x-\mu_{xg}}{\sigma_x}\right)^2+\left(\frac{y-\mu_{yg}}{\sigma_y}\right)^2-\frac{-2\rho}{\sigma_x\sigma_y}(x-\mu_{xg})(y-\mu_{yg})\right]} \tag{6.7}$$

$$LR(x,y) = \frac{f(x,y)}{g(x,y)} = e^{A_1+A_2+A_3} \tag{6.8}$$

where

$$A_1 = \frac{(\mu_{xg}-\mu_{xf})(2x-(\mu_{xf}+\mu_{xg}))}{2(1-\rho^2)\sigma_x^2} \tag{6.9}$$

$$A_2 = \frac{(\mu_{yg}-\mu_{yf})(2y-(\mu_{yf}+\mu_{yg}))}{2(1-\rho^2)\sigma_y^2} \tag{6.10}$$

$$A_3 = \frac{-\rho}{(1-\rho^2)\sigma_x\sigma_y}\left[x(\mu_{yg}-\mu_{yf})+y(\mu_{xg}-\mu_{xf})+\mu_{xf}\mu_{yf}-\mu_{xg}\mu_{yg}\right] \tag{6.11}$$

Equation 6.5 can now be evaluated numerically by sampling from the shifted distribution, calculating the Damkohler number for each sample (Figure 6.6), then the indicator function, and finally multiplying by the likelihood ratio to determine the true probabil-

ity of autoignition for the un-shifted, original distribution (Equation 6.12). It is a good sanity check to confirm that the resulting probability is independent of the magnitude of the mean shift. Figure 6.6 shows exposure to Damkohler numbers near one (indicating autoignition) are low for the original, un-shifted independent variables and crossing one for the mean-shifted independent variables.

One caveat of this importance sampling approach is that the metamodel used to generate Damkohler number for each sample must be valid for the mean-shifted inputs. This simplified example assumes validity for the alternate pressure and temperature distribution. Other IS strategies like variance modification and shifting other independents like length and radius can also serve the purpose of increasing the calculated Damkohler number to quantify autoignition risk. It is ultimately the responsibility of the designer to choose the proper alternative distribution for likelihood ratio calculation.

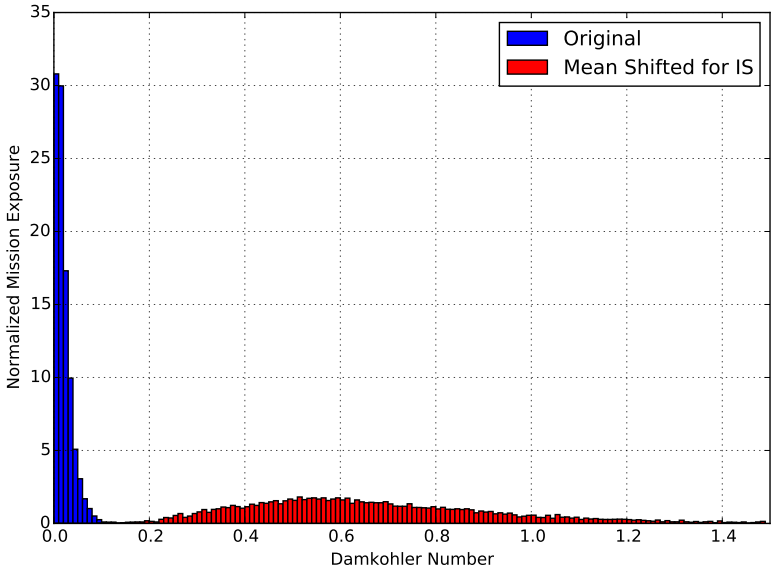

Figure 6.6: Damkohler Number Exposure for Representative Mission

$$P(A) = E_g\left[\frac{h(\mathbf{x})f(\mathbf{x})}{g(\mathbf{x})}\right] = \frac{1}{n}\sum_{i=1}^{n} h(x_i)\frac{f(x_i)}{g(x_i)} \tag{6.12}$$

For the pressure and temperature distributions outlined in Figure 6.3 and the length

Mean Radius [m]	**Mean Length [m]**	**Relative Efficiency**	**P(A)**
0.05	0.04	1.0	1.3×10^{-13}

Table 6.4: Autoignition Risk for Nominally Distributed Radius & Length

and radius distributions outlined in Figure 6.4, the probability of a Damkohler greater than one autoignition event is 4.3×10^{-13} which satisfies the requirement of $< 10^{-9}$. This result suggests there is margin to further increase efficiency by modifying the controlled length and radius parameters and still maintain an autoignition probability lower than the threshold. Table 6.4 summarizes autoignition probability for various settings of mean radius and length.

Chapter 7

Conclusions and Future Work

7.1 Results

As a result of this deterministic and stochastic analysis, additional capability has been found in the example combustion device. To maximize desirability while maintaining acceptable autoignition risk levels, the device length and radius should be retargeted to the joint distribution shown in Figure 7.1. This modified distribution is nominally 10% higher in *relative* efficiency while observing the autoignition risk threshold. The probability of autoignition for this distribution and these mission assumptions is 2.3×10^{-13}, still below the 10^{-9} limit but above the 1.3×10^{-13} nominal risk level.

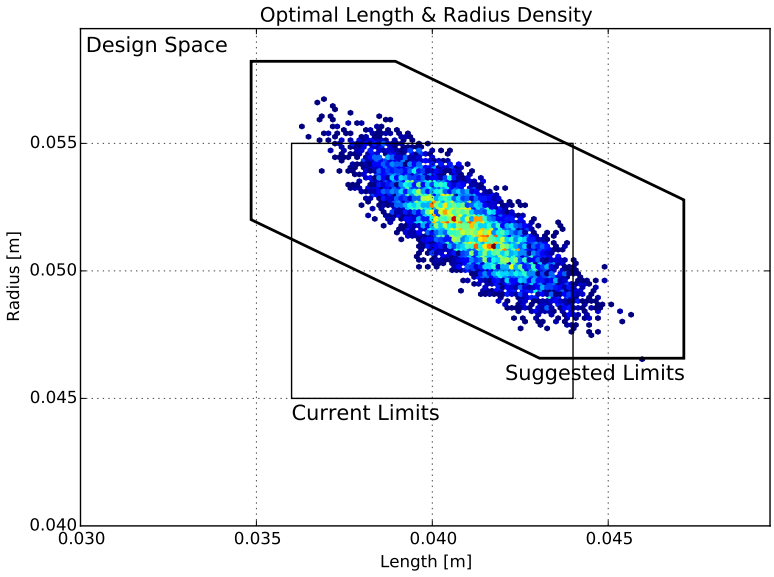

Figure 7.1: Optimal Length and Radius Target Distribution

This distribution is modified from the standard min/max tolerancing to follow the locus

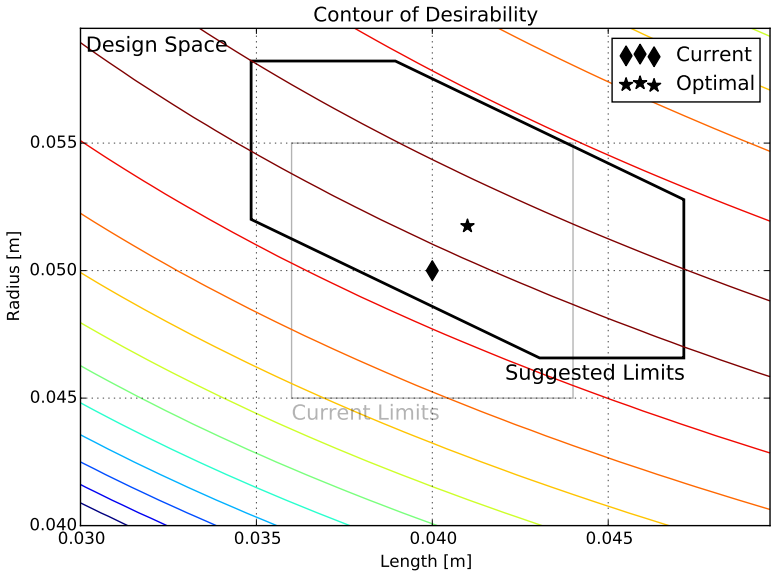

Figure 7.2: Optimal Length and Radius Desirability Contour

of maximum desirability (Figure 7.2). The manufacturing feasibility of this distribution is unknown but may be achieved with a proper hardware inspection plan. The absolute tolerances on both length and radius are larger with areas of rejection in low desirability regions. Further study of manufacturing procedures is recommended.

7.2 Procedure Summary

This work provides new contribution in the linking of importance sampling with metamodeling to provide a toolbox for deterministic and stochastic system optimization with a rare event constraint. This toolbox is outlined at a high level in the initial framework (Figure 1.1: Process Framework for Metamodel Enabled Design Optimization). The following steps are recommended in the stochastic assessment and optimization process and autoignition specific steps and assumptions are highlighted below.

1. *Determine dimensional variability in the controlled independent parameters.*

   Length and radius in the autoignition device are controllable and assumed independently and normally distributed with 2σ variance of $\pm 10\%$.

2. *Determine variability in the uncontrolled dependent parameters.*

Combustion device pressure and temperature are uncontrollable dependents relevant to autoignition. These are strongly correlated based on Brayton cycle thermodynamics and are modeled after a discretized commercial aircraft mission.

3. *Use appropriate Design of Experiment methods to conduct experiments.*

   Combustion analysis was demonstrated with 2^2 and 2^3 traditional designs. Sequential Latin hypercube was presented as an alternative. Experiment noise was simulated as a normally distributed random adder on the desirability function.

4. *Fit a metamodel to the system response.*

   Consistent with 2^2 and 2^3 traditional designs, first and second order response surfaces were fit to the combustion desirability characteristic which is obtained through separate metamodels of Damkohler and combustion efficiency characteristics.

5. *Evaluate the metamodel using standard optimization techniques to find the most desirable nominal setting for the controllable independent parameters.*

   The first and second order desirability function response surfaces were evaluated using standard optimization methodology to determine the maximum combustion desirability. An example is provided in Appendix A.

6. *In parallel, evaluate the metamodel stochastically to ensure rare event constraints are met.*

   Importance sampling techniques were used with a mean shift on the independent parameters of pressure and temperature to evaluate the Damkohler metamodel for autoignition probability.

7. *Iteratively refine the design space and repeat the metamodel fitting process with newly obtained observations.*

   This study began with first order response surfaces and progressed to second order to obtain the final deterministic optimal condition on length and radius.

8. *Propose final distribution on controllable independent parameters when design is optimized and constraints are met.*

   The bounds on length and radius were chosen to maximize the producibility of

the part, that is have the widest acceptable limits. These limits lead to a correlated distribution on length and radius which was finally evaluated via importance sampling to verify the rare event constraint is satisfied. This second round of importance sampling used the same mean shift in pressure and temperature as the first round.

Metamodeling is the tool to tie all of these pieces together. Proper Design of Experiment feeds into metamodeling and deterministic optimization and importance sampling then evaluate the metamodel. Without a metamodel, these optimization and stochastic evaluations would be prohibitively expensive. Metamodels enable this entire process to be iterative and progress through these iterations faster. As iterations progress, metamodel fidelity increases further guiding the next round of experiments. These steps efficiently combine Design of Experiments, metamodeling, and stochastic simulation to reduce the number of design iterations without losing accuracy. The above steps show the unification of metamodeling and rare event analysis and capture the new contributions of this work.

7.3 Recommendations

There is also residual value in the now high accuracy and fast executing metamodel. This metamodel can be applied beyond the design process in service use applications such as on-board diagnostics. The metamodel can be used as the foundation for a self-improving algorithm that observes the system in the background while gathering data on normal operating characteristics. The algorithm may then alert the operator when abnormal characteristics are observed or take independent action to correct the error or safely shut down the system to prevent catastrophic damage. The emerging industry trends toward "big data" and analytics emphasize the importance of accurate and fast metamodels.

Several extensions of this work specific to the autoignition application have been identified. Higher fidelity in chemical time stochastic assessment can be obtained by including local fuel stoichiometry variation though its influence on t_{chem} is low. A more accurate hardware representation will benefit both the deterministic and stochastic assessment. This accuracy can be gained using CFD to simulate actual operating conditions with actual

hardware to observe the effects of swirling flow, device wall contouring, and elliptical deformation on calculated residence time of a particle from injection to exit. Finally, chemical reaction simulation software can examine in detail the complex, multi-step mechanisms in combustion of hydrocarbons. This software can accurately predict the pressure rise signature of autoignition [3]. The drawbacks of this software include significant calculation time and limited hardware modeling options. Metamodeling is an ideal technique to link these complex software packages.

In summary, this work outlined an iterative approach to assess a current design (controllable independents) in its current environment (uncontrollable independents) against a rare event requirement while maximizing system desirability. Metamodeling is the enabling link between DoE, deterministic optimization, and stochastic analysis for rare events. Weaknesses of metamodeling, such as extrapolation, must be understood and respected. Wider use of appropriate metamodeling in all stages of the design process will drive efficiency in experiment and result in higher performing products. Use of metamodeling outside of the design process carries benefits many are just beginning to realize.

Appendix A

Optimization Example Problem

A.1 Problem Description

To test the validity of various optimization approaches, a very simple two dimensional problem is used to show several ways to determine the optimal system inputs to achieve the desired system output. From Vakili [22], the simple function is of the form:

$$J(\mathbf{x}) = (\mathbf{x} - \mathbf{a})^T Q(\mathbf{x} - \mathbf{a}) + c \tag{A.1}$$

where $\mathbf{x}$ is the column vector of inputs, $\mathbf{a}$ is a given column vector, Q is a positive definite matrix and c is a scalar.

$$\mathbf{a} = \begin{pmatrix} 3 \\ 8 \end{pmatrix} \quad Q = \begin{pmatrix} 2 & 1 \\ 1 & 2 \end{pmatrix} \quad c = 3 \tag{A.2}$$

The objective is to minimize the response $J(\mathbf{x})$ with a unique optimal response at $\mathbf{a}$ as shown in Figure A.1 [22].

In practical design applications, the form of the response is rarely known and is often accompanied by some error in the observed value from the true response. To model this simply, a normally distributed noise term will be added.

$$Y(\mathbf{x}) = Y(\mathbf{x}) + \epsilon(\mathbf{x}) \tag{A.3}$$

Where the noise term has mean zero and variance four. The noise is assumed to be independent of the function.

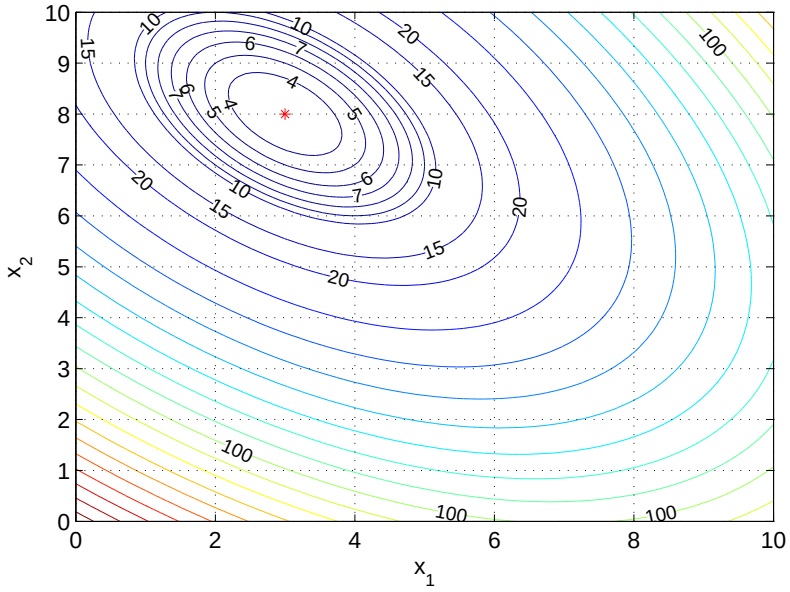

Figure A.1: Contour of response $J(\mathbf{x})$

$$\epsilon(\mathbf{x}) \sim \mathcal{N}(\mu, \sigma^2) \sim \mathcal{N}(0, 4) \tag{A.4}$$

Since the functional form of the system is not known to the designer, the design optimization process must be conducted through experiment and observation. To replicate realistic constraints, an experiment budget is set of 50 (then 100) sampling points. These points can be unique or replicates but the total number of observations must not exceed the allotted budget. A comparison is made between several techniques to determine the best approach for optimizing a noisy system within the experiment budget.

A.2 Sequential Design of Experiment Optimization

The first approach to determining the optimal response is to begin at a point in the design space and experiment around it using traditional design of experiment theory. For this problem, there are two controllable variables and they are set at two levels. From the origin, the experiment is conducted at a positive x_1 step, a negative x_1 step, a positive x_2 step, and a negative x_2 step. From this observed (noisy) data, a linear regression model

is fit and the direction of steepest descent is obtained. The center of the next round of experimentation is proportional to the regression coefficients from the first round as shown in Figure A.2 [13]. This procedure is repeated with each round using four experiments from the budget until the budget is exhausted or a sufficient optimal point is found.

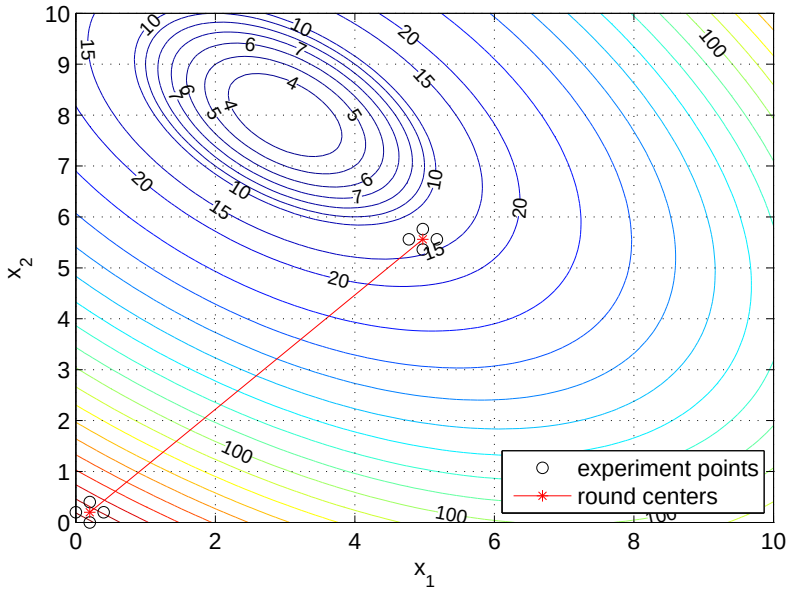

Figure A.2: Experiment locations for round 1 and round 2.

The results in Figure A.3.1 show that sequential steepest descent optimization using a linear regression model at each round is sufficient to determine the optimal system input for the noise-free case.

Noise complicates the optimization process because noise influences the four experiments per round and may drive the calculated path of steepest descent far away from the true path of steepest descent as shown in Figure A.3.2. For a budget of 50 experiments, the end point is far away from the optimal point. As the budget of experiments is increased (Figure A.3.3 and Figure A.3.4), the behavior is still erratic but approximately averages out to the optimal point.

It is important to note that the noise assumption for this sample problem is a normally distributed adder with mean zero and variance equal to 4. This noise is assumed

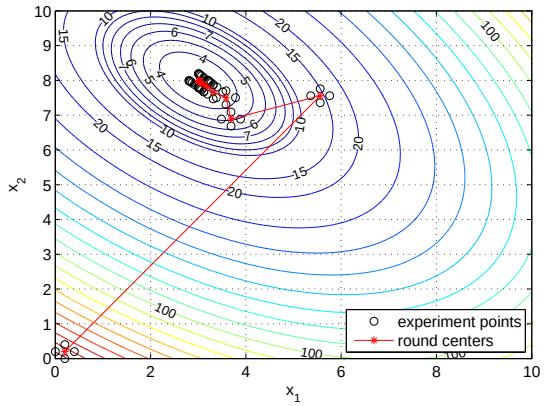

A.3.1: 50 experiments with no noise, $x_1 = 3$, $x_2 = 8$

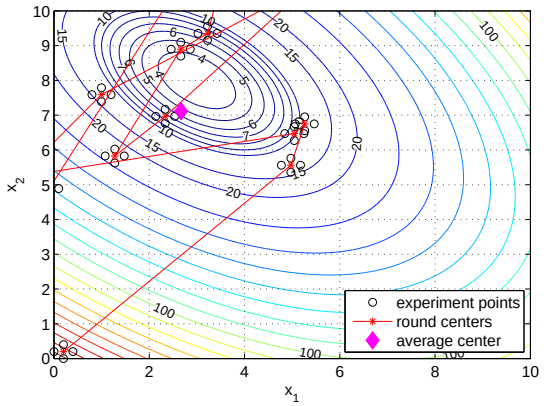

A.3.2: 50 experiments with noise, $x_1 = 2.7$, $x_2 = 7.1$

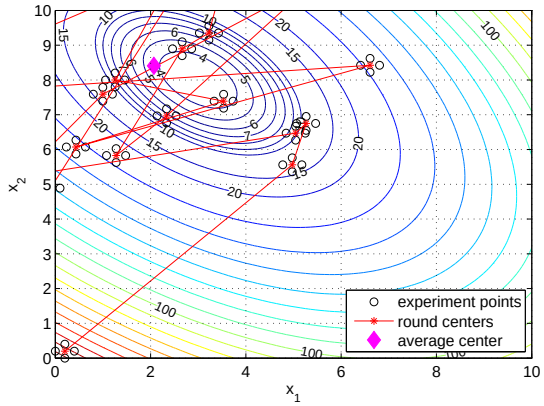

A.3.3: 100 experiments with noise, $x_1 = 2.1$, $x_2 = 8.4$

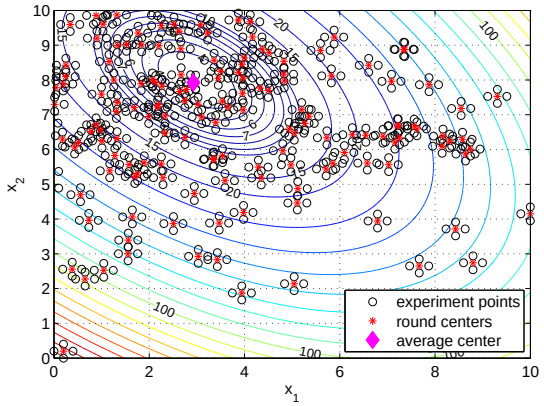

A.3.4: 1000 experiments with noise, $x_1 = 2.9$, $x_2 = 7.9$

Figure A.3: Experiment locations in the design space.

independent of the control variables and system output. This is significant because near the optimal location, the magnitude of the response is nearly the same as the variance. This means that for a given sampling round of four experiments, the closer to the optimal, the harder it is to discern noise from true function. If the noise were proportional to the response, this sequential steepest descent method may find a optimal point faster. Another technique to reduce the influence of noise is to replicate experiments within the current round. This uses the experiment budget faster but may also lead to faster and more robust convergence on the optimal.

A.3 Metamodel Driven Optimization

A second approach is enabled by metamodeling techniques to create a mathematical representation of the design space based on a limited number of observations and optimize on the metamodel instead of the system. For the first, simplest example, a Gaussian Process (Kriging) based metamodel is fit to 25 noisy observations from the response described in A.1. The 25 experiments are conducted at an evenly spaced grid of points in the design space. The metamodel is then sampled at a very fine resolution in the same design space and the minimum is taken as the optimal point for the original system.

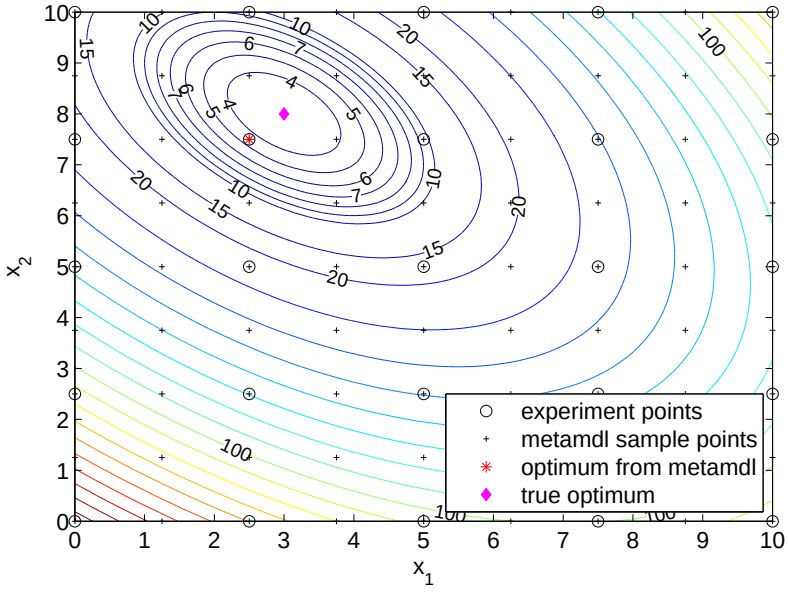

Figure A.4: 25 experiment locations with metamodel samples, optimal $x_1 = 2.5$,$x_2 = 7.5$.

The optimal point is determined solely by the resolution of the metamodel sampling grid. This sampling can be done sequentially with little computational penalty. The sampling grid resolution is determined by optimal sufficiency or how close is close enough.

In addition to sequential metamodel sampling, the designer can experiment sequentially until the budget is exhausted. The first round of 25 experiments serves as a screening round to narrow the design space in which a second experiment round can be conducted. The metamodel fitting after the second round should also include the observations from the first

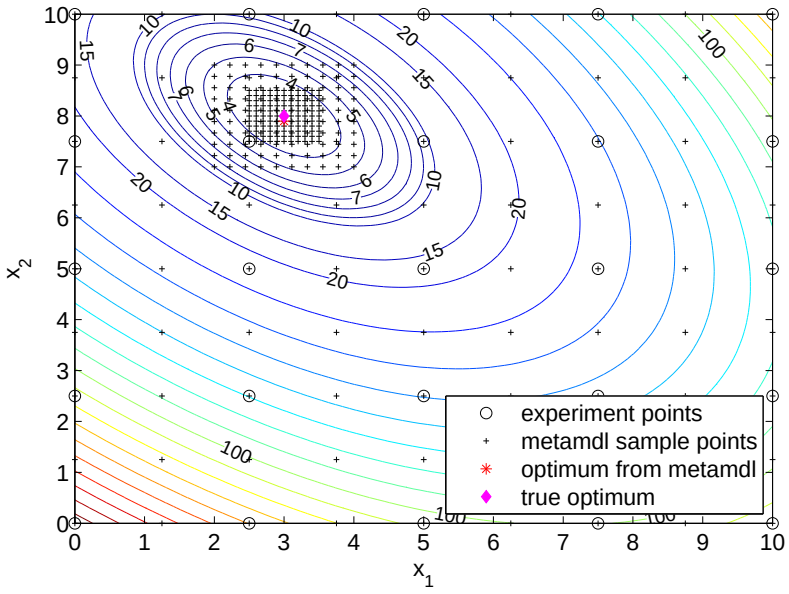

Figure A.5: 25 experiments with sequential metamodel samples, optimal $x_1 = 3.0$,$x_2 = 7.9$.

round to build the most robust metamodel. This second metamodel can then be sampled at high resolution and sequentially (Figure A.7) until the desired accuracy in the optimum is achieved. This whole process can go on ad infinitum unless otherwise constrained by budget or desired accuracy.

Experiment efficiency can also be increased using randomized experiment and metamodel sampling techniques such as Latin hypercube.

The kriging method to generate the above metamodel uses the properties of joint normal distributions between the observed response (y) and predicted response ($y_\star$).

$$\begin{bmatrix} \mathbf{y} \\ \mathbf{y}_\star \end{bmatrix} \sim \mathcal{N}\left(\begin{bmatrix} \mu \\ \mu_\star \end{bmatrix}, \begin{bmatrix} K(X,X) + \sigma^2 I & K\left(X, X_\star\right) \\ K\left(X_\star, X\right) & K\left(X_\star, X_\star\right) + \sigma^2 I \end{bmatrix} \right) \tag{A.5}$$

where (X) is the vector of independents for the known responses, $(X_\star)$ is the vector of independents for the unknown responses and $K()$ is the kernel function that relates the covariance between the known and unknown independents. The characteristic length term (ℓ) is chosen by the user for best model fit. This can be determined iteratively using the

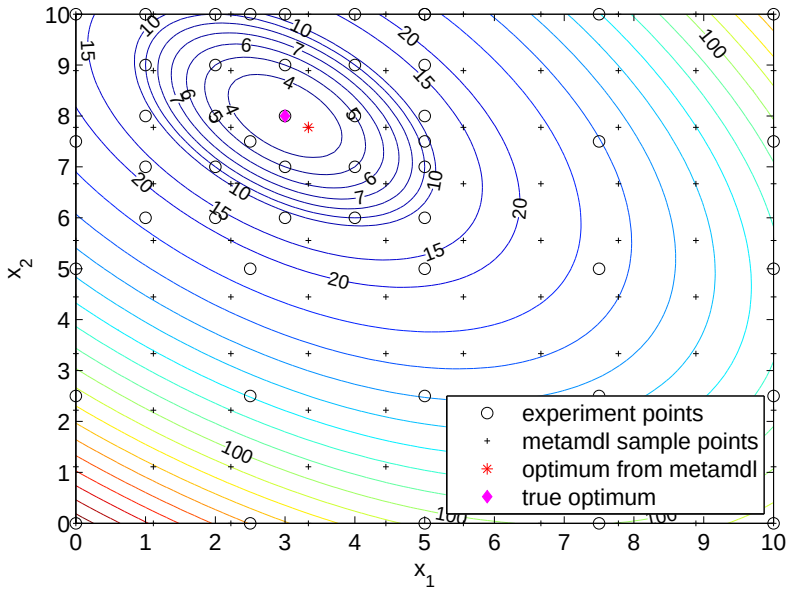

Figure A.6: 50 experiments in two sequential sets of 25 (2x25), optimal $x_1 = 3.3$,$x_2 = 7.8$.

leave-k-out metamodel validation technique. For this simplified study, $\ell = 1.2$.

$$\operatorname{cov}\left(f(\mathbf{x}), f(\mathbf{x}')\right) = K(\mathbf{x}, \mathbf{x}') = \exp\left(-\frac{1}{2\sqrt{\ell}}|\mathbf{x} - \mathbf{x}'|^2\right) \tag{A.6}$$

Finally, the mean and variance of the unknown response can be written as

$$\mathbf{M} = \mu_\star + CA^{-1}\left(\mathbf{y} - \mu\right) \tag{A.7}$$

$$= \mu_\star + K\left(X_\star, X\right) K\left(X, X\right)^{-1}\left(\mathbf{y} - \mu\right) \tag{A.8}$$

$$\mathbf{V} = B - CA^{-1}C^\top \tag{A.9}$$

$$= \left[K\left(X_\star, X_\star\right) + \sigma^2 I\right] - K\left(X_\star, X\right)\left[K\left(X, X\right) + \sigma^2 I\right]^{-1} K\left(X, X_\star\right) \tag{A.10}$$

where $\mu = \mu_\star = 0$ as a kriging best practice.

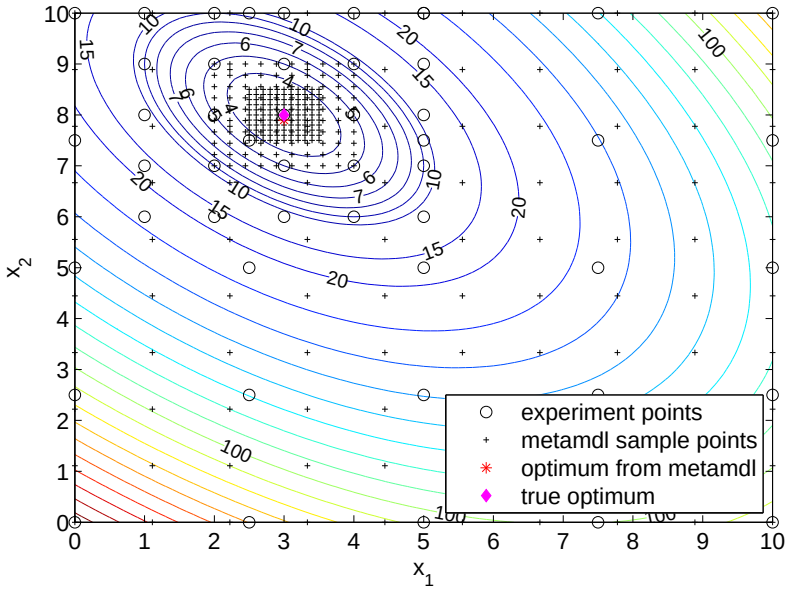

Figure A.7: 50 (2x25) experiments with sequential metamodel samples, optimal $x_1 = 3.0$,$x_2 = 7.9$.

Appendix B

Select Statistical Techniques

B.1 Metamodel Samples Residual Normality Plots

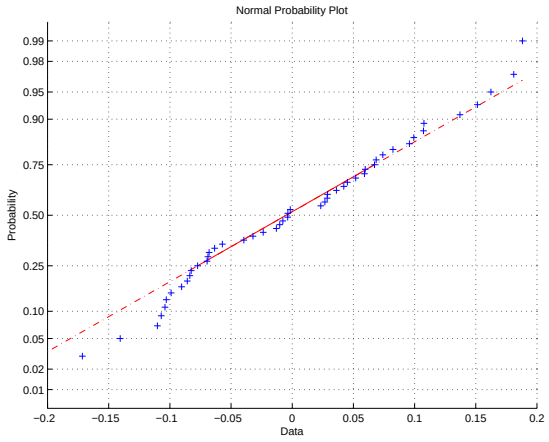

B.1.1: Linear RSM

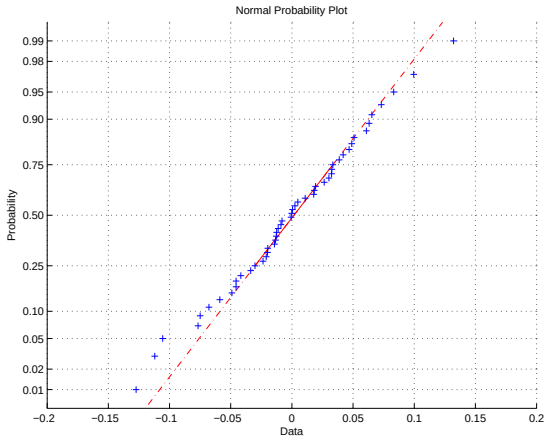

B.1.2: Second Order RSM

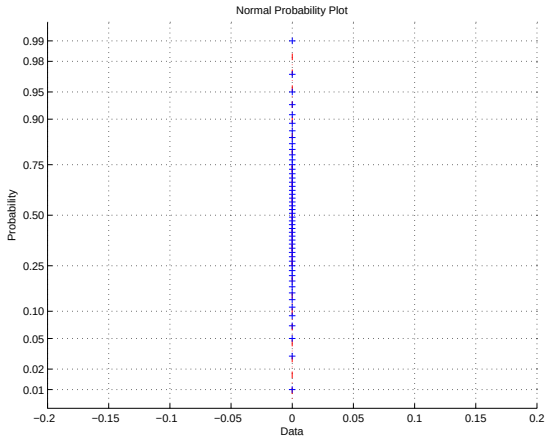

B.1.3: RBF

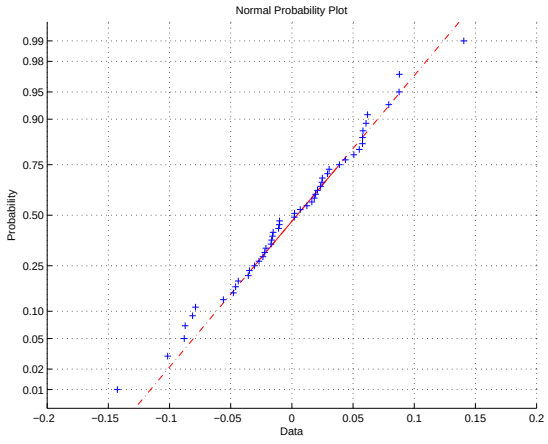

B.1.4: Kriging

Figure B.1: Residual Normality Plots for $y = x^2 + \epsilon$

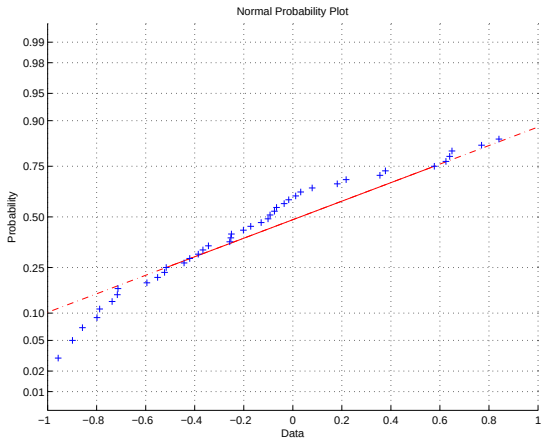

B.2.1: Linear RSM

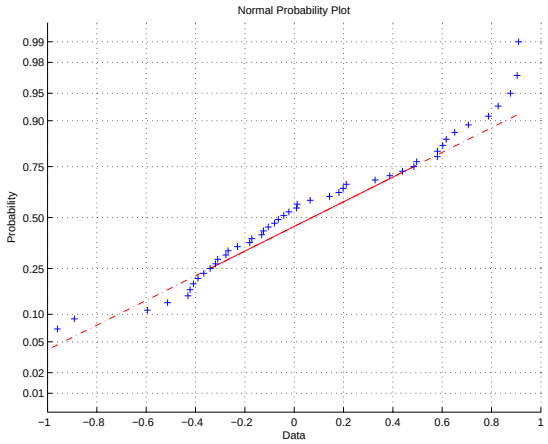

B.2.2: Second Order RSM

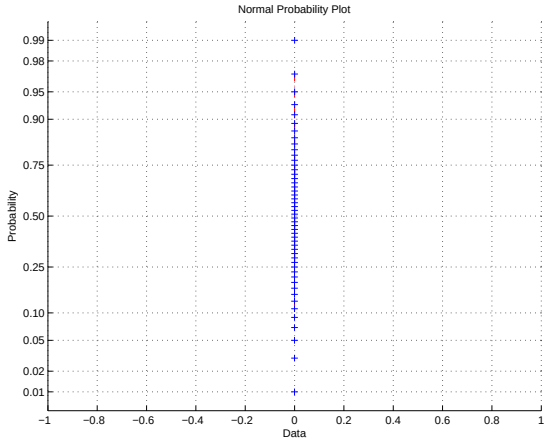

B.2.3: RBF

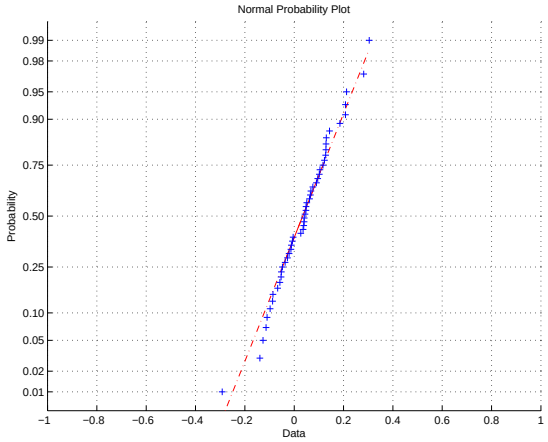

B.2.4: Kriging

Figure B.2: Residual Normality Plots for $y = 2\sqrt{x} + \cos(x) + \epsilon$

B.2 Rare Event Sample Size

If the true probability of a rare event is $p = 10^{-9}$, the central limit theorem allows an estimate of that probability ($\hat{p}$) to be written as a normally distributed random variable since the number of samples is very large ($n \gg 1$). [18]. A 95% confidence interval can then be established around the estimate using a standard normal z-value of 1.96.

$$p = \hat{p} \pm \frac{1.96\sigma}{\sqrt{n}} \tag{B.1}$$

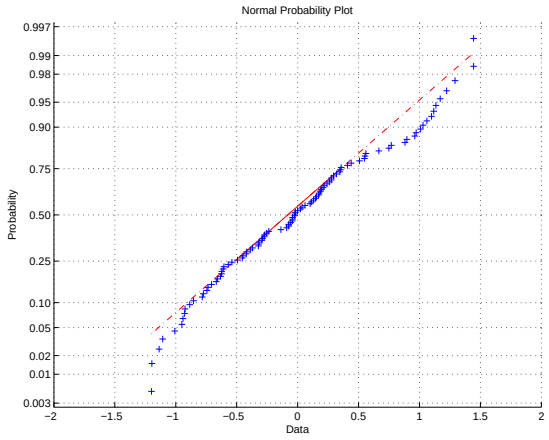

B.3.1: Linear RSM

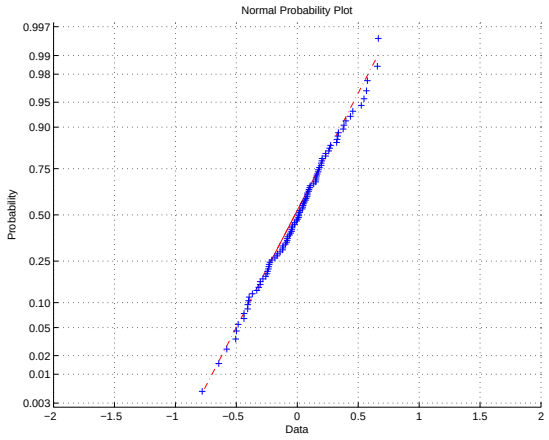

B.3.2: Second Order RSM

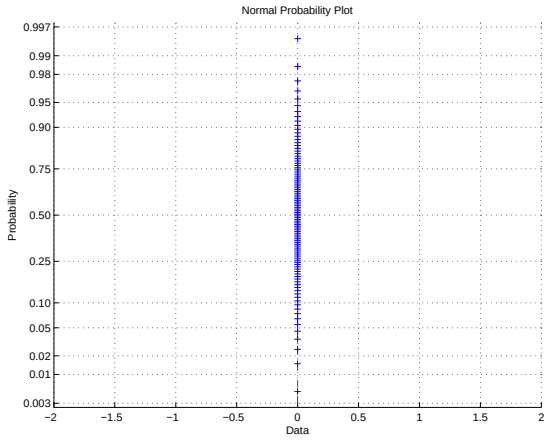

B.3.3: RBF

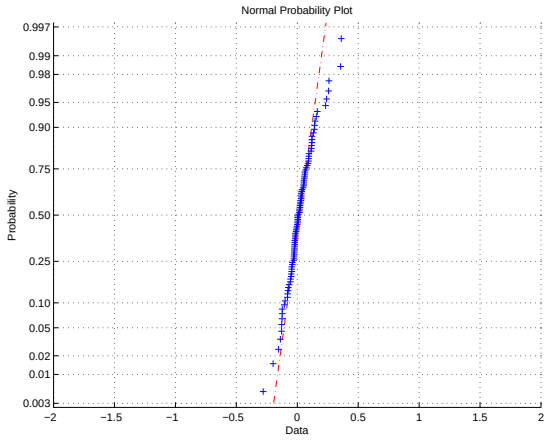

B.3.4: Kriging

Figure B.3: Residual Normality Plots for $y = \sqrt{x_1} + \sqrt{x_2} + \cos(x_1) + \cos(x_2) + \epsilon$

Since the true variance (σ^2) of the probability is not known, it is estimated (without bias) with

$$\hat{\sigma}^2 = \frac{n\hat{p}\,(1-\hat{p})}{(n-1)} \tag{B.2}$$

$$p = \hat{p} \pm \frac{1.96}{\sqrt{n}} \sqrt{\frac{n\hat{p}\,(1-\hat{p})}{(n-1)}} \tag{B.3}$$

$$p = \hat{p} \pm \frac{1.96}{\sqrt{n-1}} \sqrt{\hat{p}\,(1-\hat{p})} \tag{B.4}$$

For very small values of probability, the absolute error $(p - \hat{p})$ isn't as meaningful as the relative error [18].

$$RE = \frac{(p - \hat{p})}{p} \tag{B.5}$$

A meaningful relative error is based on the confidence interval α

$$RE = 2\,(1 - \alpha) = 0.1 = 10\% \tag{B.6}$$

Rewriting Equation B.4 in terms of relative error

$$RE = 0.1 \geq \frac{(p - \hat{p})}{p} = \frac{1.96}{\sqrt{n-1}} \frac{\sqrt{\hat{p}\,(1 - \hat{p})}}{p} \tag{B.7}$$

Since $\hat{p}$ is very close to zero, $(1 - \hat{p}) \approx 1$

$$0.1 \geq \frac{1.96}{\sqrt{n-1}} \frac{\sqrt{\hat{p}}}{p} \tag{B.8}$$

$$0.1 \geq \frac{1.96}{\sqrt{(n-1)}\sqrt{p}} \tag{B.9}$$

Rearranging for n

$$\sqrt{(n-1)} \geq \frac{1.96}{0.1\sqrt{p}} \tag{B.10}$$

$$n \geq \frac{1.96^2}{0.1^2 p} + 1 \tag{B.11}$$

To satisfy a minimum failure criteria of one event in 10^9 opportunities with 95% confidence, the number of samples must be greater than 3.84×10^{11} or 384 billion samples.

$$n \geq 384,160,000,001 \tag{B.12}$$

Bibliography

[1] G. E. P. Box and J. S. Hunter. Multi-factor experimental designs for exploring response surfaces. *The Annals of Mathematical Statistics*, pages 195–241, 1957.

[2] Y. A. Cengel and M. A. Boles. *Thermodynamics: An Engineering Approach*. McGraw-Hill Series in Mechanical Engineering. McGraw-Hill Higher Education, 2005.

[3] Reaction Design. *CHEMKIN Software Manual*. San Diego. 10112, 2011.

[4] A. Donato and R. Pitchumani. Quicker: Quantifying uncertainty in computational knowledge engineering rapidly. *Powder Technology*, 265:54–65, 2014.

[5] A. A. Giunta. *Aircraft Multidisciplinary Design Optimization Using Design Of Experiments Theory And Response Surface Modeling Methods*. PhD thesis, Virginia Polytechnic Institute, 1997.

[6] A. H. Lefebvre and D. R. Ballal. *Gas Turbine Combustion: Alternative Fuels and Emissions, Third Edition*. Taylor & Francis, 2010.

[7] A.H. Lefebvre, W. Freeman, and L. Cowell. *Spontaneous Ignition Delay Characteristics of Hydrocarbon Fuel Air Mixtures*. Purdue University. NASA Contractor Report, February 1986.

[8] C. J. Marek, L. C. Papathakos, and P. W. Verbulecz. Preliminary studies of autoignition and flashback in a premixing-prevaporizing flame tube using jet-a fuel at lean equivalence ratios. *NASA TM*, X-3526:13, 1977.

[9] J. D. Mattingly. *Elements of Propulsion: Gas Turbines and Rockets*. AIAA education series. American Institute of Aeronautics and Astronautics, 2006.

[10] D. N. Mavris, O. Bandte, and D. A. DeLaurentis. Robust design simulation: A probabilistic approach to multidisciplinary design. *Journal of Aircraft*, 36(1):298–307, 1999.

[11] D. N. Mavris, D. A. DeLaurentis, O. Bandte, and M. A. Hale. A stochastic approach to multi-disciplinary aircraft analysis and design. In *36th Aerospace Sciences Meeting & Exhibit, Reno, NV*, 1998.

[12] M. Meckesheimer, A. J. Booker, R. R. Barton, and T. W. Simpson. Computationally inexpensive metamodel assessment strategies. *AIAA journal*, 40(10):2053–2060, 2002.

[13] D. C. Montgomery. *Design and Analysis of Experiments*. Wiley, 2005.

[14] R. H. Myers, D. C. Montgomery, and C. M. Anderson-Cook. *Response Surface Methodology: Process and Product Optimization Using Designed Experiments*. Wiley Series in Probability and Statistics. Wiley, 2009.

[15] W. H. Press, S. A. Teukolsky, W. T. Vetterling, and B. P. Flannery. *Numerical Recipes 3rd Edition: The Art of Scientific Computing*. Cambridge University Press, 2007.

[16] C. E. Rasmussen and C. K. I. Williams. *Gaussian Processes for Machine Learning (Adaptive Computation and Machine Learning)*. The MIT Press, 2006.

[17] S. M. Ross. *Simulation*. Elsevier Science, fifth edition, 2012.

[18] G. Rubino and B. Tuffin. *Rare Event Simulation using Monte Carlo Methods*. Wiley, 2009.

[19] T. W. Simpson, J. D. Poplinski, P. N. Koch, and J. K. Allen. Metamodels for computer-based engineering design: survey and recommendations. *Engineering With Computers*, 17(2):129–150, 2001.

[20] R. R. Tacina. Autoignition in a premixing-prevaporizing fuel duct using three different fuel injection systems at inlet air temperatures to 1250 k. *NASA TM*, 82938:13, 1983.

[21] S. R. Turns. *An Introduction to Combustion: Concepts and Applications*. McGraw-Hill Series in Mechanical Engineering. McGraw-Hill, 2000.

[22] P. Vakili. Design optimization. Personal Communication, 06 Dec 2014.

[23] P. Vakili. Likelihood ratio normal. Personal Communication, 10 Mar 2014.

[24] S. S. Vasu, D. F. Davidson, and R. K. Hanson. Jet fuel ignition delay times: Shock tube experiments over wide conditions and surrogate model predictions. *Combustion and Flame*, 152(12):125 – 143, 2008.

[25] G. Gary Wang and S. Shan. Review of metamodeling techniques in support of engineering design optimization. *Journal of Mechanical Design*, 129(4):370 – 380, 2006.

[26] L. Wang, D. Beeson, G. Wiggs, and M. Rayasam. A comparison of meta-modeling methods using practical industry requirements. *47th AIAA/ASME/ASCE/AHS/ASC Structures, Structural Dynamics, and Materials Conference*, AIAA 2006-1811, 4 May 2006.

Curriculum Vitae

Contact Paul Morrison

pauljmorrison@outlook.com

Department of Mechanical Engineering, Boston University, 110 Cummington Mall, Boston, MA 02215, USA

Education

Boston University M.Sc. candidate, September 2004 – present. Thesis advisor: Pirooz Vakili.

University of Cincinnati, B.Sc., Mechanical Engineering, September 2008 – June 2011.

Youngstown State University, Mechanical Engineering, September 2005 – September 2008.

Experience

GE Aviation, *Lynn, MA*. Turbofan / Turbojet Performance Engineering. June 2011 – present.

GE Aviation, *Cincinnati, OH*. GEnx Performance Engineering Intern. June 2010 – June 2011.

GE Aviation, *Cincinnati, OH*. Combustion Design Intern. May 2008 – March 2010.